[redacted]

Copy 6
RM L53F08

[redacted]

NACA

RESEARCH MEMORANDUM

FLIGHT MEASUREMENTS OF LIFT AND DRAG FOR THE BELL X-1 RESEARCH AIRPLANE HAVING A 10-PERCENT-THICK WING

By Edwin J. Saltzman

Langley Aeronautical Laboratory
Langley Field, Va.

NATIONAL ADVISORY COMMITTEE
FOR AERONAUTICS

WASHINGTON

September 3, 1953

[redacted]

NATIONAL ADVISORY COMMITTEE FOR AERONAUTICS

RESEARCH MEMORANDUM

FLIGHT MEASUREMENTS OF LIFT AND DRAG FOR THE BELL X-1 RESEARCH AIRPLANE HAVING A 10-PERCENT-THICK WING

By Edwin J. Saltzman

SUMMARY

Drag coefficients have been determined during power-off transonic flight for the Bell X-1 airplane having a 10-percent-thick wing over the Mach number range from 0.68 to 1.01 at pressure altitudes from 22,000 to 49,000 feet. The lift-coefficient range investigated extended to maximum lift for Mach numbers up to 0.89 and to values above 0.5 for the remainder of the test range. These data are compared with flight data for the X-1 airplane having an 8-percent-thick wing and with wind-tunnel data for the airplane having a 10-percent-thick wing.

The results indicate that the lift curves are flat-topped beyond maximum lift coefficient for Mach numbers to 0.89, the highest speed at which maximum lift was reached. The angle of attack necessary to achieve maximum lift is near 9° for Mach numbers from 0.68 to 0.81 and increases to 15° at a Mach number of 0.89. The drag-rise Mach number decreases with increasing lift from 0.80 at a lift coefficient of 0.2 to 0.74 at a lift coefficient of 0.6. At a lift coefficient of 0.4 the drag coefficient at sonic speed is about 5.6 times the value at Mach number of 0.75.

Comparison with the 8-percent-thick-wing flight data indicates that in the range of Mach number where data are comparable, Mach number of 0.78 to 0.89, the 10-percent-thick-wing airplane had slightly lower maximum lift coefficients. Comparison also shows that the thicker wing encounters the drag rise earlier, about 0.03 to 0.06 in Mach number, and experiences a one-third greater increase in drag coefficient from subcritical to sonic speeds. The lift-drag ratios for the thicker wing airplane are 75 to 85 percent of those for the 8-percent-thick-wing airplane at the speed of sound; and the drag coefficient at zero lift for the thick-wing airplane is 20 to 40 percent greater than for the thin-wing airplane at Mach numbers beyond the drag rise. The induced drag factor for the 10-percent-thick-wing airplane is greater than for the 8-percent-thick-wing airplane at Mach numbers between 0.76 and 0.91, being about twice as high at Mach numbers from 0.83 to 0.88. The flight-test data for the 10-percent-thick wing are in good agreement with the wind-tunnel measurements.

INTRODUCTION

As a part of the Air Force-Navy-NACA high-speed flight research program, lift and drag coefficients have been determined for the Bell X-1 (10-percent-thick wing) airplane during power-off transonic flight. The results are presented in this paper. Comparisons with flight data for the X-1 (8-percent-thick wing) airplane (ref. 1) and wind-tunnel data for the X-1 (10-percent-thick wing) airplane (ref. 2) are included. Earlier less extensive drag measurements for both 10-percent-thick-wing and 8-percent-thick-wing airplanes for power-on and power-off flight have been reported in reference 3.

SYMBOLS

A_X	longitudinal acceleration, g units
A_Z	normal acceleration, g units
C_D	drag coefficient
C_{D_O}	drag coefficient at zero lift
C_L	lift coefficient
C_N	normal-force coefficient
C_X	longitudinal-force coefficient
g	acceleration due to gravity, ft/sec^2
M	Mach number
M_{DR}	drag-rise Mach number, Mach number where $dC_D/dM = 0.1$
q	dynamic pressure, lb/sq ft
R	Reynolds number
S	wing area, sq ft
W	airplane weight, lb

[redacted]

$dC_L/d\alpha$ lift-curve slope

dC_D/dC_L^2 induced drag factor

α angle of attack, deg

Subscript:

max maximum

AIRPLANE AND INSTRUMENTATION

The general physical characteristics of the airplane are given in table I and a three-view drawing is shown in figure 1.

Standard NACA recording instruments were used to determine impact and static pressure, longitudinal and normal acceleration, and angle of attack. All records were synchronized by a common timer. Impact and static pressures were measured approximately 0.6 maximum fuselage diameter ahead of the fuselage nose. The angle-of-attack vane was located about 17 inches forward of the fuselage nose and 7 inches to the left of the fuselage center line. The airspeed calibration was obtained with the aid of an Askania phototheodolite and an NACA modified SCR 584 radar set by using the method of reference 4.

METHODS

The accelerometer method was used to determine normal and longitudinal forces. The force coefficients were computed from

$$C_N = WA_Z/qS$$

$$C_X = WA_X/qS$$

Lift and drag coefficients were computed from

$$C_L = C_N \cos \alpha - C_X \sin \alpha$$

$$C_D = C_X \cos \alpha + C_N \sin \alpha$$

[redacted]

ACCURACY

The estimated accuracy of the measured quantities is:

Mach number	±0.01
Normal acceleration, g units	±0.05
Longitudinal acceleration, g units	±0.015
Airplane weight, percent	±1.0
Angle of attack:	
Instrument and reading accuracy, deg	±0.05
Vane floating (a zero shift), deg	0.40

The estimated zero shift due to vane floating and the following references to angle-of-attack error are based on reference 5. Error due to boom bending can be considered negligible because of the short distance from the fuselage nose to the vane axis, 17 inches. Error due to boom upwash was neglected because the ratio of the distance between boom axis and vane to the boom radius should cause an error of less than 2 percent according to figure 10 of reference 5. A positive error due to upwash ahead of the wing and fuselage is known to exist in determining angle of attack. The magnitude of this error has not been determined experimentally for a wing and fuselage combination such as the X-1 airplane. Results of an investigation for a specific swept-wing fighter-type airplane are available (ref. 5); but in view of the vast difference between the X-1 airplane and the specific configuration of reference 5, and because of a general over-all lack of upwash information, corrections cannot be safely applied to the present data.

A theoretical estimate of wing upwash error has been made and is briefly discussed in reference 1 where the magnitude of this error is estimated to be about 7 percent at subsonic speeds. Theoretically the error approaches zero at sonic and supersonic speeds. However, at present there is not a satisfactory theoretical method for predicting fuselage upwash and because of the uncertainty of applying wing upwash corrections while ignoring the fuselage contribution, corrections were omitted in reference 1 and in the present paper.

TESTS

Lift and drag data were recorded during level flight, pull-ups, turns, and push-overs at pressure altitudes from 22,000 to 49,000 feet and for a Mach number range from 0.68 to 1.01. Reynolds number varied from 4.3×10^6 to 14.7×10^6 based on the mean aerodynamic chord. All data were obtained in power-off flight.

RESULTS AND DISCUSSION

Present Data

The variations of lift and drag coefficients with angle of attack for various Mach numbers are presented in figure 2. These data indicate that the angle of attack necessary for maximum lift remains near 9° from $M = 0.68$ to $M = 0.81$ and then increases with Mach number to about 15° at $M = 0.89$ beyond which speed $C_{L_{max}}$ was not obtained because of the rapid increase in $C_{L_{max}}$ as sonic speed is approached and the difficulty of maintaining speed during these maneuvers. Figures 2 and 3 indicate that maximum lift coefficient decreases as Mach number is increased from $M = 0.68$ to $M \approx 0.81$ and then increases with Mach number, reaching 0.84 at $M = 0.89$. At higher Mach numbers the angle of attack for maximum lift was not exceeded, although lift coefficients as high as 1.0 were reached.

The variation of lift coefficient with Mach number for constant angles of attack is shown in figure 3. At angle of attack of 4°, a peak C_L value of approximately 0.6 is attained between Mach numbers of 0.72 and 0.79; and a low C_L value of about 0.4 is reached at $M = 0.89$.

The effect of Mach number on $dC_L/d\alpha$ as obtained from figure 2 is also presented in figure 3. Peak values are obtained near $M = 0.77$ and $M = 0.94$ ($C_L = 0.2$ to 0.4), with a maximum of approximately 0.10 at Mach number of 0.77. The value of $dC_L/d\alpha$ reaches a minimum of 0.07 for this lift range at $M = 0.89$. These lift-curve slopes are directly affected by changing errors in determining angle of attack. The wing and fuselage upwash produces changing errors which tend to reduce the computed value of the lift-curve slope. Because applicable upwash data are not available, the degree of consequent error in $dC_L/d\alpha$ values cannot be stated. The section entitled "Comparisons" and figure 13 relate the lift-curve slopes of flight and wind-tunnel tests for the 10-percent-thick-wing airplane.

Figure 4 presents the variation of C_D with Mach number for constant values of lift coefficient. The drag-rise Mach number decreases with lift from about $M = 0.80$ for $C_L = 0.2$ to about $M = 0.74$ for $C_L = 0.6$. For $C_L = 0.4$ the drag coefficient at $M = 1.0$ increases to approximately 5.6 times its value at $M = 0.75$.

The change in lift-drag ratio with Mach number for constant C_L values is given in figure 5. The maximum lift-drag ratio is approximately

3.2 at the speed of sound for a lift coefficient near 0.6. At $M = 0.75$ maximum L/D is about 14.5 for a lift coefficient near 0.4.

Comparisons

Figures 6 to 12 present a comparison of the results of the present investigation with flight tests of the X-1 airplane having an 8-percent-thick wing as reported in reference 1, and with wind-tunnel tests of an X-1 model having a 10-percent-thick wing as reported in reference 2.

Flight data for 10-percent-thick wing and 8-percent-thick wing.- A comparison of the variation of $C_{L_{max}}$ with Mach number for the two airplanes is shown in figure 6. For the Mach number range where data can be compared, $M = 0.78$ to 0.89, the maximum lift coefficient of the 10-percent-thick wing is slightly lower than for the 8-percent-thick wing.

The variation of C_D with Mach number for constant lift coefficients of 0.2, 0.4, and 0.6, shown in figure 7, indicates that M_{DR} is 0.03 to 0.06 lower for the 10-percent-thick wing than for the airplane having the 8-percent-thick wing. For the thick-wing airplane the increase in drag coefficient from subcritical to sonic speeds is about one-third greater than that for the thin-wing airplane.

Figure 8 presents a comparison of the variation of L/D with Mach number at constant lift coefficient for the two data sources. At Mach numbers above 0.75, the value of L/D for the 10-percent-thick wing is lower than for the thinner wing. The lift-drag ratios at sonic speeds for the 10-percent-thick-wing airplane are 75 to 85 percent of those for the 8-percent-thick wing.

Figure 9 shows the effect of Mach number on C_{D_0}. Extrapolation of data from figure 2 and corresponding data from reference 1 indicates that the drag coefficient at zero lift for the 10-percent-thick-wing airplane is 20 to 40 percent greater than for the thinner wing X-1 at Mach numbers beyond the drag rise. The variation of the induced drag factor dC_D/dC_L^2 with Mach number is also compared in figure 9. These slopes are average values for lift coefficients between 0.3 and 0.4. The slope values for both X-1 airplanes are similar up to $M \approx 0.76$ where the induced drag factor for the thicker wing increases, reaching values approximately double that of the 8-percent-thick wing between $M = 0.83$ and $M = 0.88$. The values of dC_D/dC_L^2 are approximately equal at speeds above $M = 0.91$.

Flight and wind-tunnel data for 10-percent-thick wing.- Figures 10 and 11 present the variation of C_D and L/D, respectively, with Mach

number for constant lift coefficients. Agreement between the two data sources is satisfactory except at the lowest Mach numbers where the drag determination in flight is least accurate. The Reynolds number range for the 1/16-scale tunnel model is 1.03×10^6 to 1.80×10^6 as compared with 4.3×10^6 to 14.7×10^6 for the flight data.

Figure 12 consists of the variation of drag coefficient at zero lift with Mach number and the variation of the induced drag factor with Mach number. The agreement is favorable for the Mach number range covered.

The lift-curve slope for the 10-percent-thick-wing airplane is presented in figure 13. The sources of data, full-scale flight, 1/16-scale wind tunnel (ref. 2), and 1/4-scale wind tunnel (unpublished), display similar variations with Mach number but vary in magnitude of $dC_L/d\alpha$. As has been previously mentioned, the changing upwash error in measuring angle of attack would tend to reduce the computed flight values of the lift-curve slope. The effects of the balancing tail loads on $dC_L/d\alpha$ are slight. Reynolds numbers for the three data sources are included in the figure.

CONCLUDING REMARKS

The following results were obtained for the Bell X-1 airplane having a 10-percent-thick wing from power-off flight tests covering the Mach number range 0.68 to 1.01:

1. The angle of attack necessary to obtain maximum lift coefficient remains near 9° for Mach numbers from 0.68 to 0.81 and increases to 15° at a Mach number of 0.89, the highest Mach number at which maximum lift coefficient was obtained. The lift curves are flat beyond maximum lift coefficient.

2. The drag-rise Mach number is approximately 0.80 at a lift coefficient of 0.2 and decreases to about 0.74 at a lift coefficient of 0.6. The drag coefficient is approximately 5.6 times greater at sonic speed than at a Mach number of 0.75 for a lift coefficient of 0.4.

3. The maximum lift-drag ratio is approximately 3.2 at sonic speed for a lift coefficient near 0.6.

The following are results of the comparison of the 10- and 8-percent-thick-wing flight data and the 10-percent-thick-wing tunnel data:

1. The maximum lift coefficient of the 10-percent-thick wing is slightly lower than for the 8-percent-thick wing for the Mach number range where data can be compared.

2. The drag rise for the thicker wing airplane occurs 0.03 to 0.06 lower in Mach number than for the thinner wing X-1 airplane.

3. The drag-coefficient increase from subcritical to sonic speeds for the 10-percent-thick-wing airplane is about one-third greater than the increase experienced by the 8-percent-thick-wing airplane.

4. Lift-drag ratios for the 10-percent-thick wing are 75 to 85 percent of those for the thinner wing at sonic speeds.

5. The drag coefficient at zero lift for the 10-percent-thick-wing airplane is 20 to 40 percent greater than for the 8-percent-thick-wing X-1 airplane at Mach numbers above the drag rise.

6. The value of the induced drag factor for the 10-percent-thick-wing airplane is approximately double the value for the 8-percent-thick-wing airplane between Mach numbers of 0.83 to 0.88. Above a Mach number of 0.91 the slopes are about equal.

7. The 10-percent-thick-wing flight and wind-tunnel drag results are in good agreement.

Langley Aeronautical Laboratory,
National Advisory Committee for Aeronautics,
Langley Field, Va., May 20, 1953.

[redacted]

REFERENCES

1. Carman, L. Robert, and Carden, John R.: Lift and Drag Coefficients for the Bell X-1 Airplane (8-Percent-Thick Wing) in Power-Off Transonic Flight. NACA RM L51E08, 1951.

2. Mattson, Axel T., and Loving, Donald L.: Force, Static Longitudinal Stability, and Control Characteristics of a 1/16-Scale Model of the Bell XS-1 Transonic Research Airplane at High Mach Numbers. NACA RM L8A12, 1948.

3. Gardner, John J.: Drag Measurements in Flight on the 10-Percent-Thick and 8-Percent-Thick Wing X-1 Airplanes. NACA RM L8K05, 1948.

4. Zalovcik, John A.: A Radar Method of Calibrating Airspeed Installations on Airplanes in Maneuvers at High Altitudes and at Transonic and Supersonic Speeds. NACA Rep. 985, 1950. (Supersedes NACA TN 1979.)

5. McFadden, Norman M., Holden, George R., and Ratcliff, Jack W.: Instrumentation and Calibration Technique for Flight Calibration of Angle-of-Attack Systems on Aircraft. NACA RM A52I23, 1952.

TABLE I

PHYSICAL CHARACTERISTICS OF THE BELL X-1 AIRPLANE

HAVING A 10-PERCENT-THICK WING

Airplane:	
Power plant:	
Four-unit rocket engine	Reaction Motors, Inc. model 6000C4
Rated sea-level thrust per unit, lb	1500
Weight:	
Full (approximately), lb	12,400
Empty, lb	7270
Wing:	
Airfoil section	NACA 65-110 (a = 1)
Area (including section through fuselage), sq ft	130
Span, ft	28
Aspect ratio	6
Mean aerodynamic chord, ft	4.81
Root chord, ft	6.18
Tip chord, ft	3.09
Incidence:	
Root, deg	2.5
Tip, deg	1.5
Sweepback at leading edge, deg	5.05
Dihedral (chord plane), deg	0
Horizontal tail:	
Airfoil section	NACA 65-008
Area, sq ft	26
Span, ft	11.4
Aspect ratio	5
Vertical tail:	
Area (excluding dorsal fin), sq ft	25.6

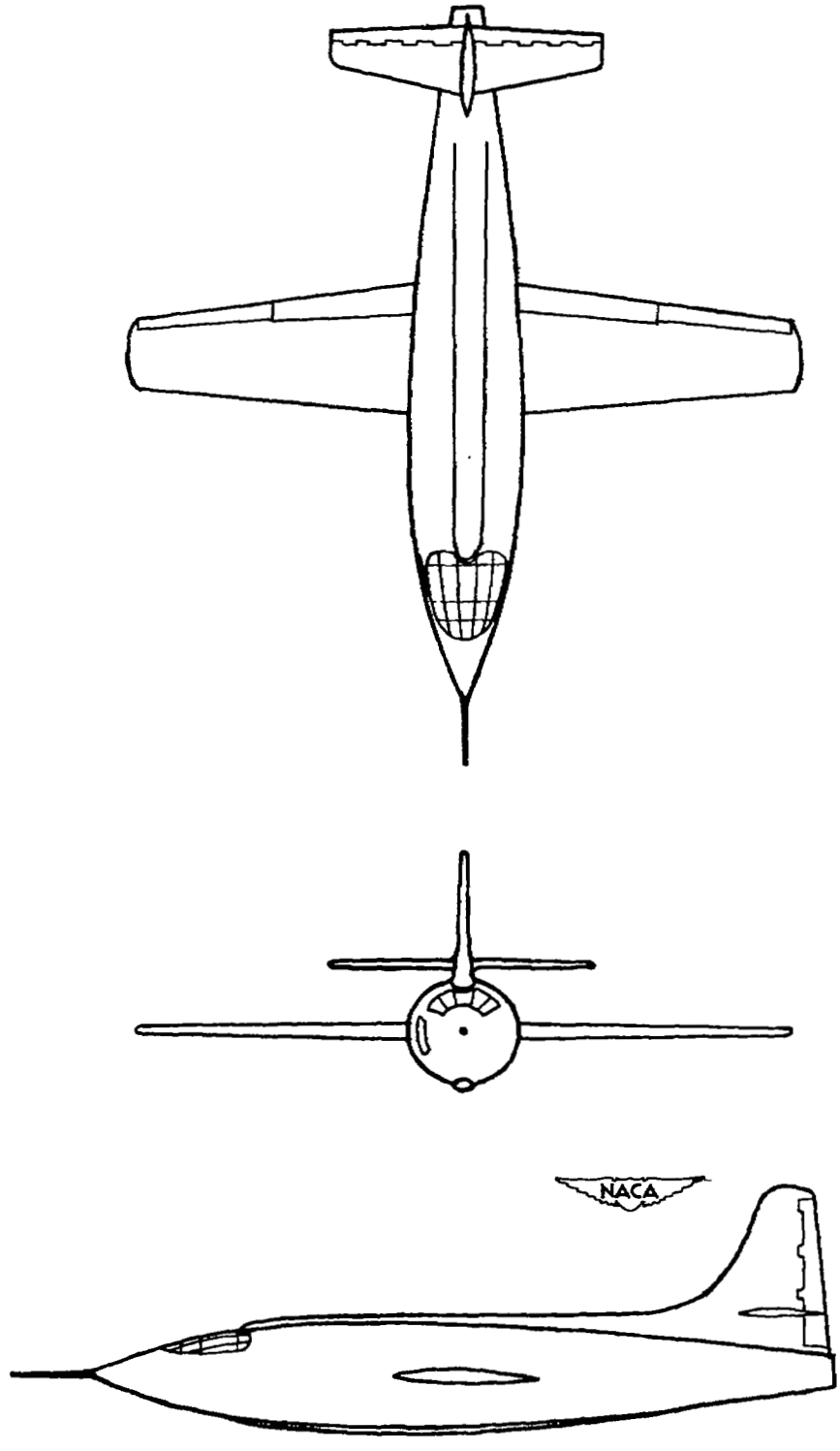

Figure 1.- Three-view drawing of the Bell X-1 airplane.

[redacted]

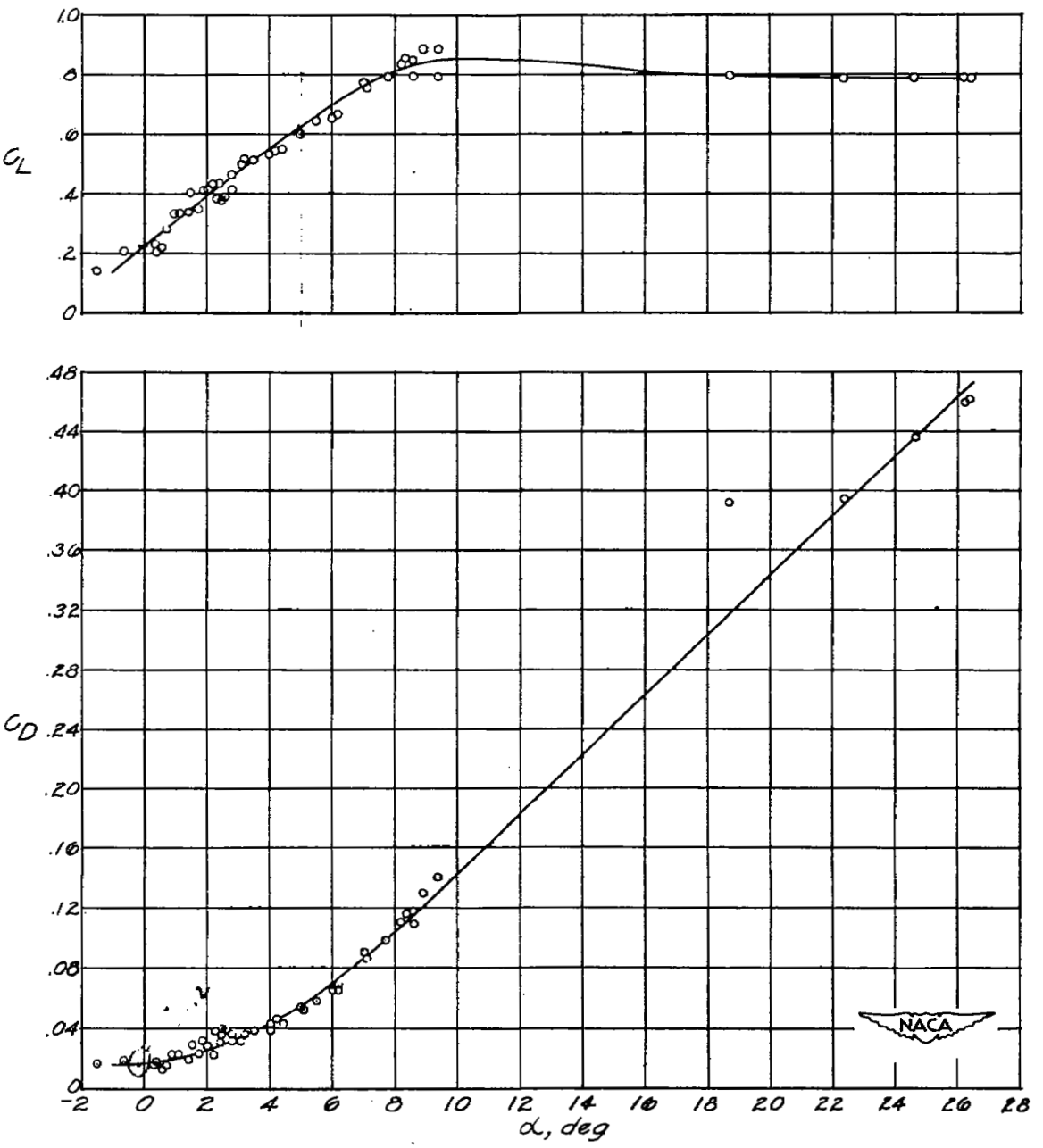

(a) M = 0.68.

Figure 2.- Variation of lift coefficient and drag coefficient with angle of attack for constant Mach number.

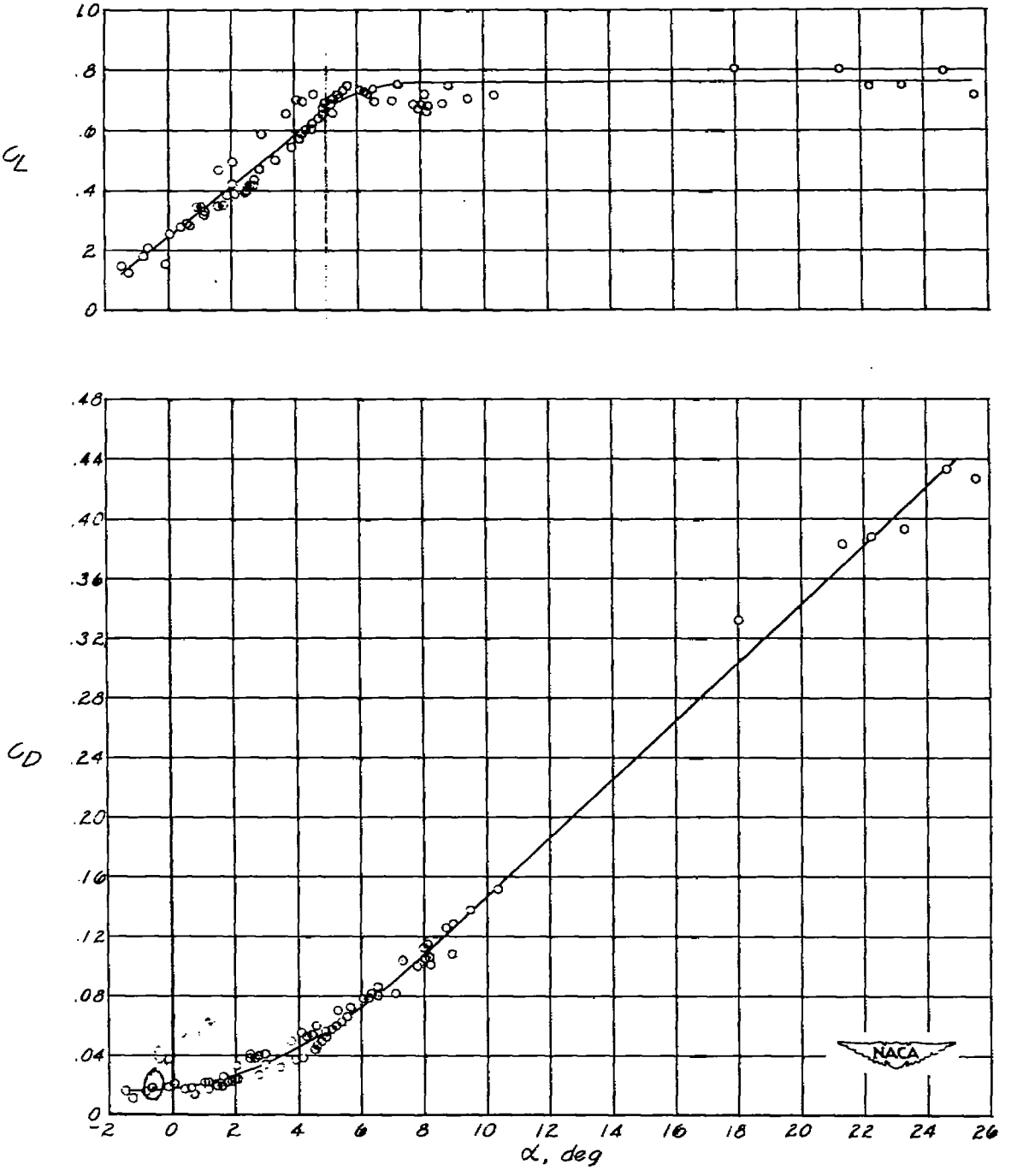

(b) M = 0.71.

Figure 2.- Continued.

[redacted]

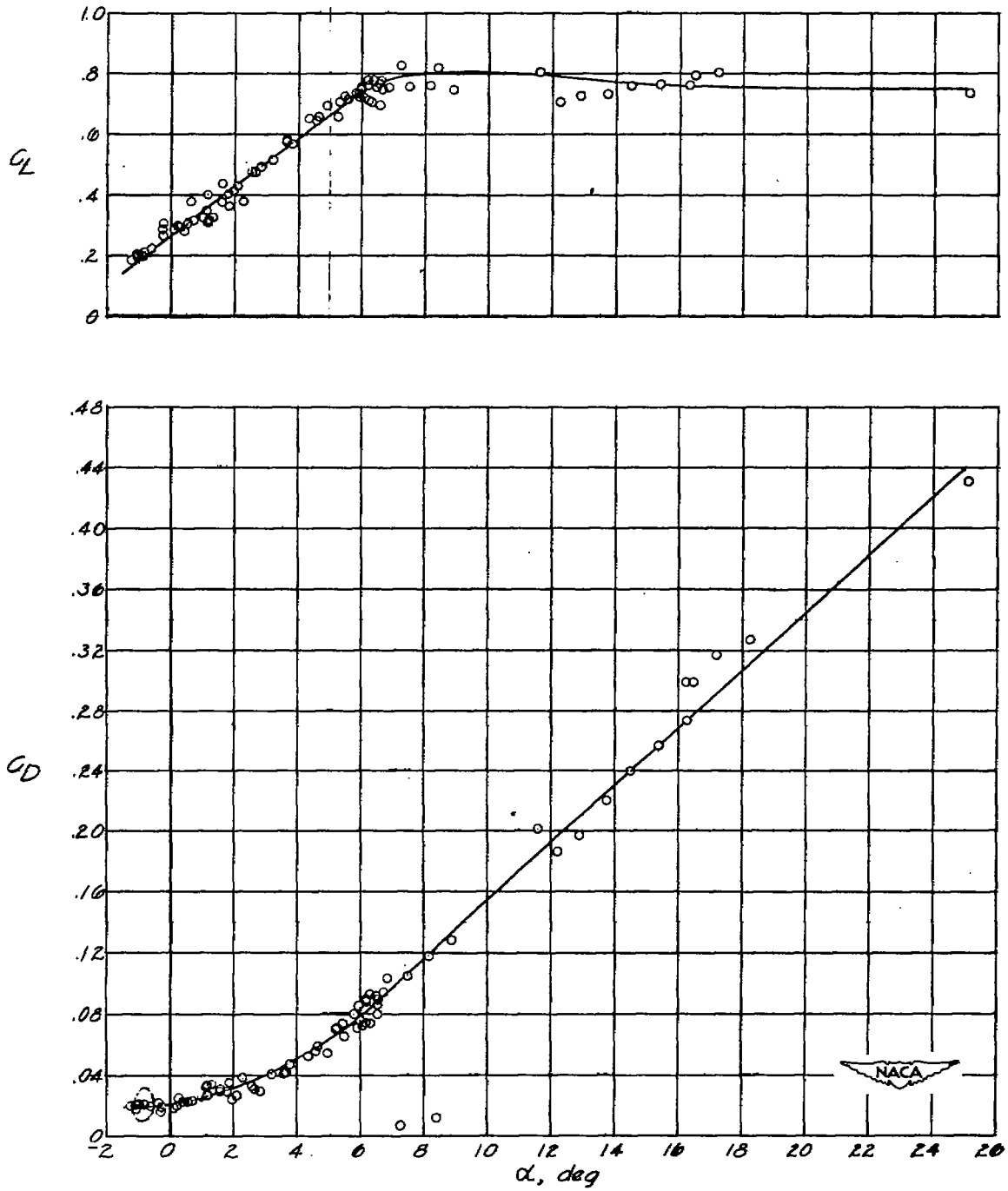

(c) M = 0.73.

Figure 2.- Continued.

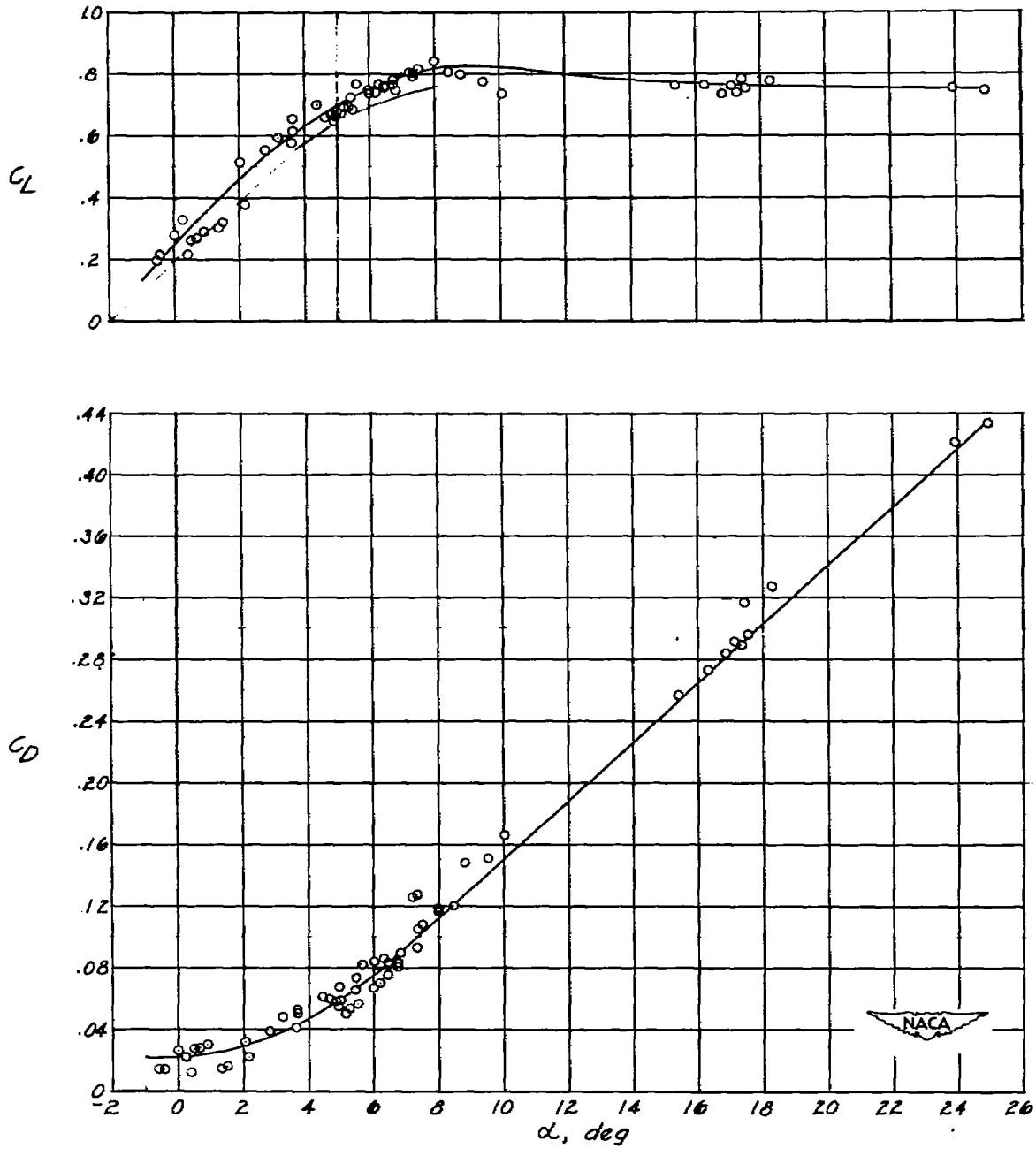

(d) M = 0.75.

Figure 2.- Continued.

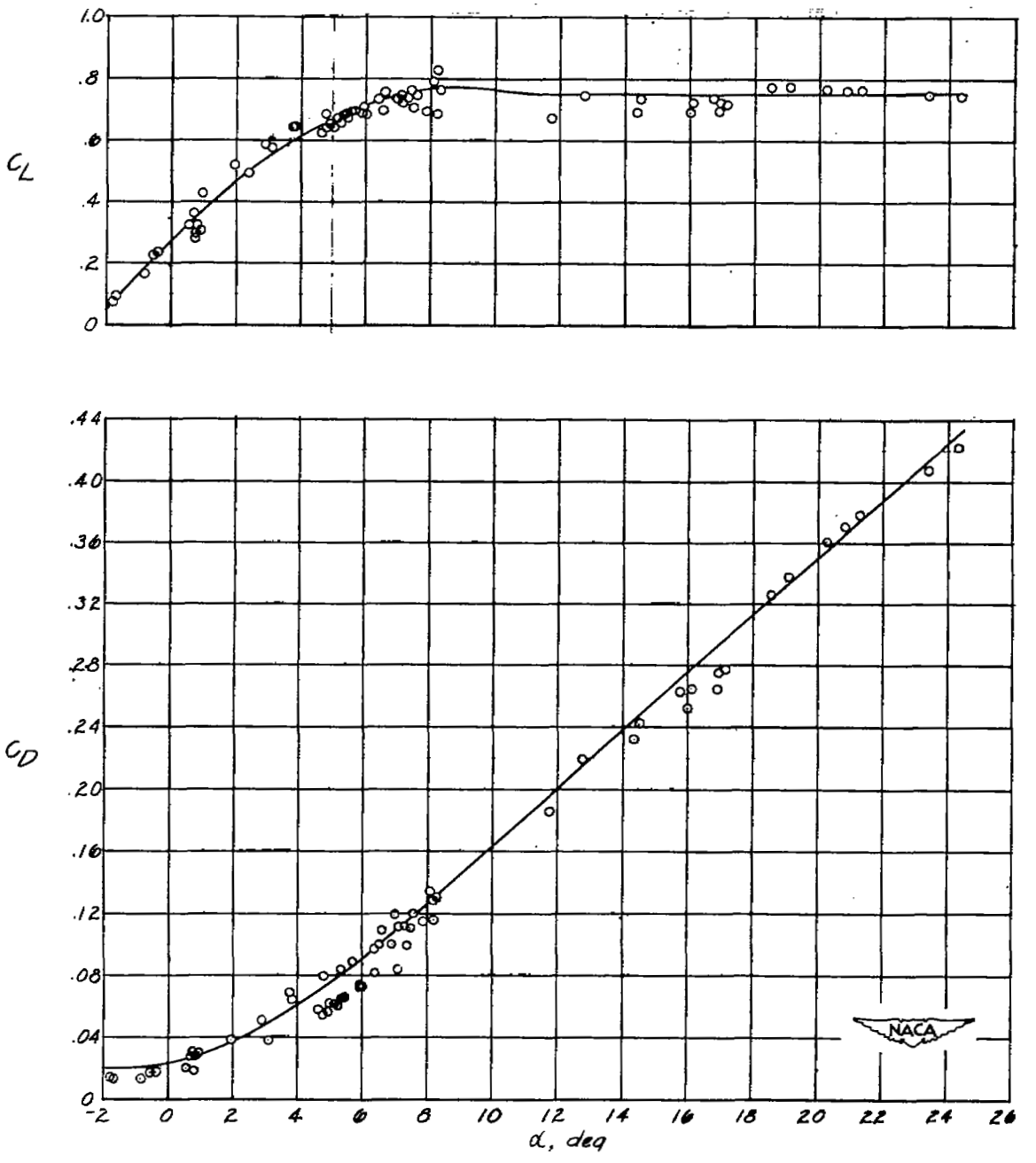

(e) M = 0.77.

Figure 2.- Continued.

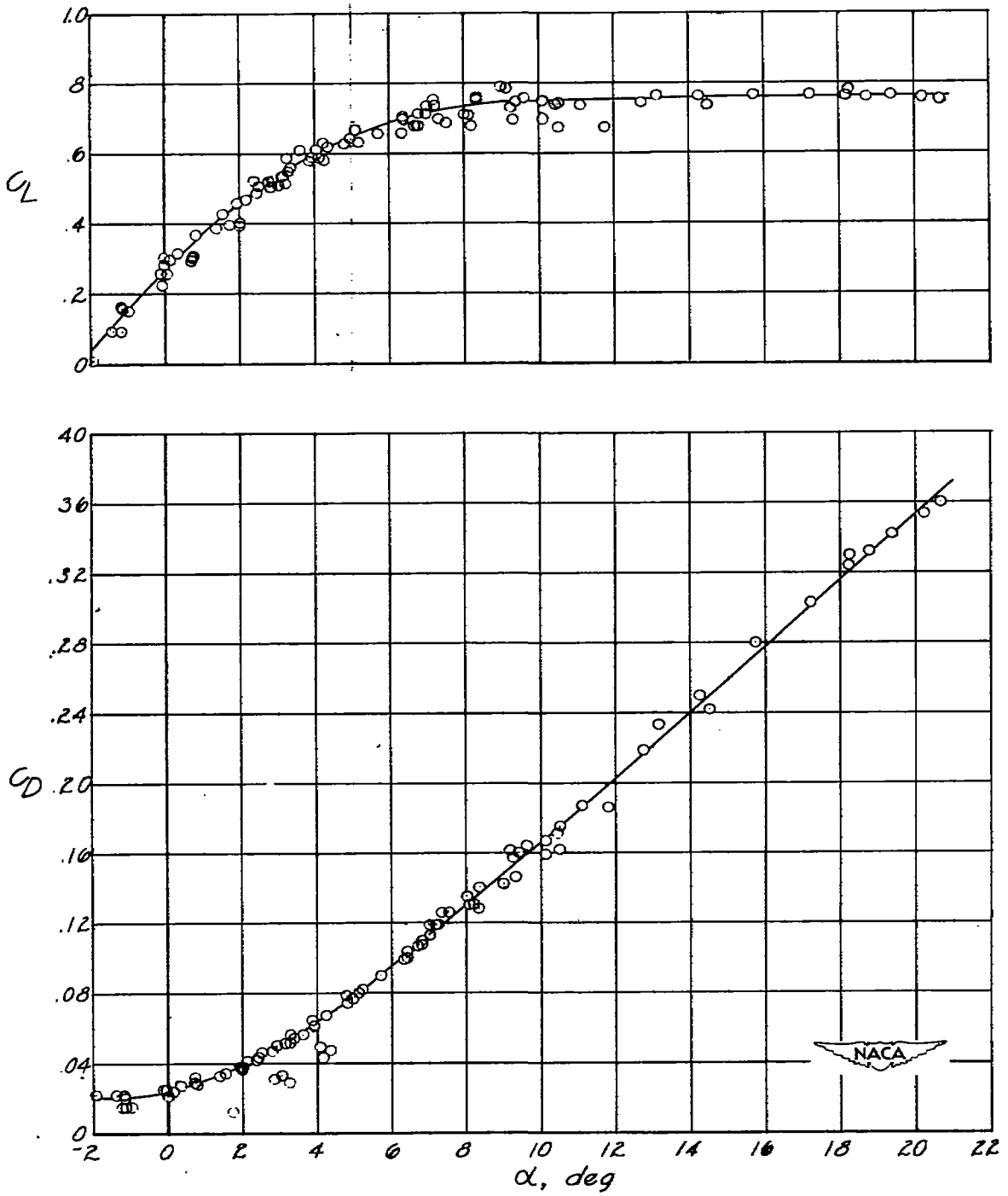

(f) M = 0.79.

Figure 2.- Continued.

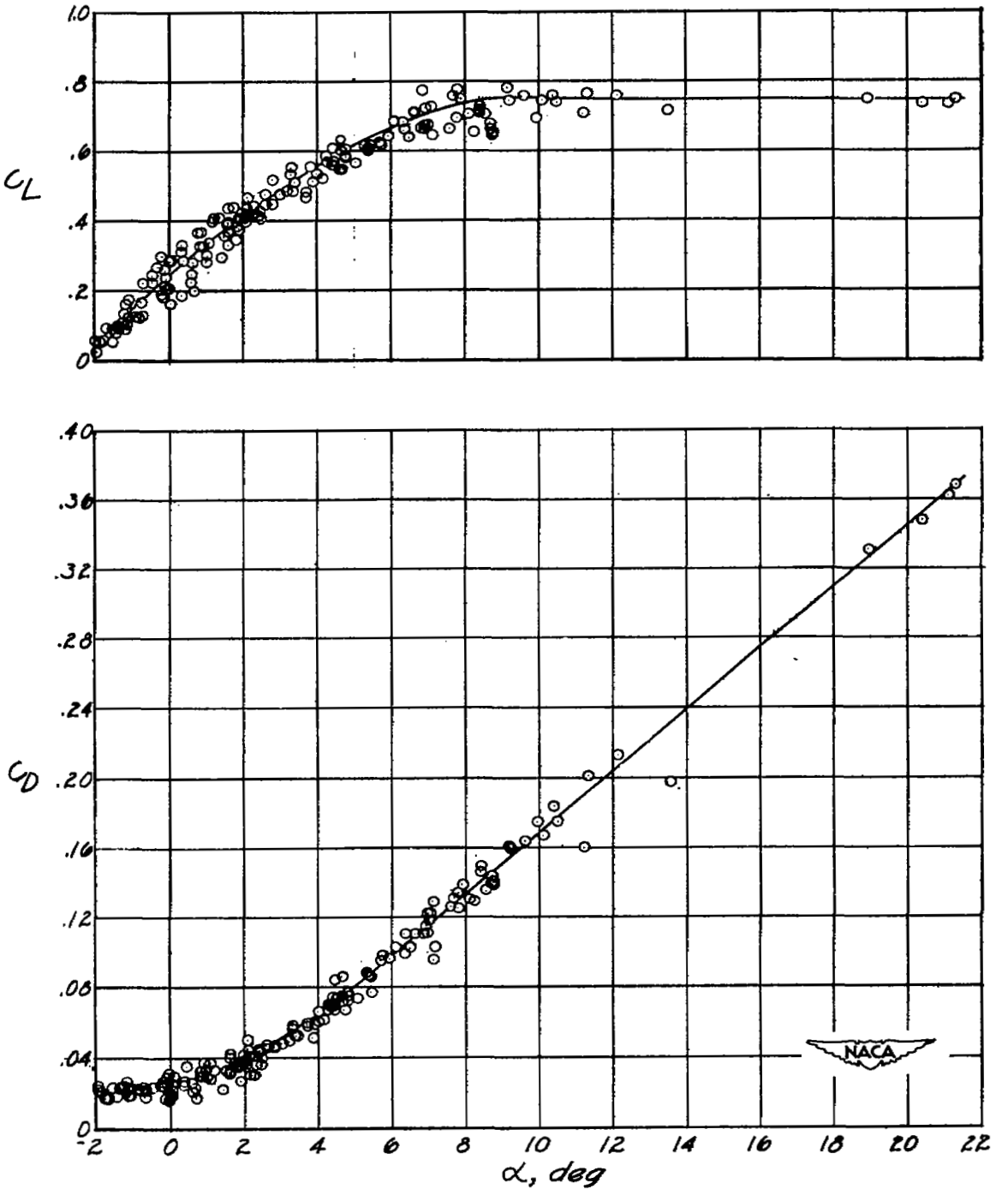

(g) M = 0.81.

Figure 2.- Continued.

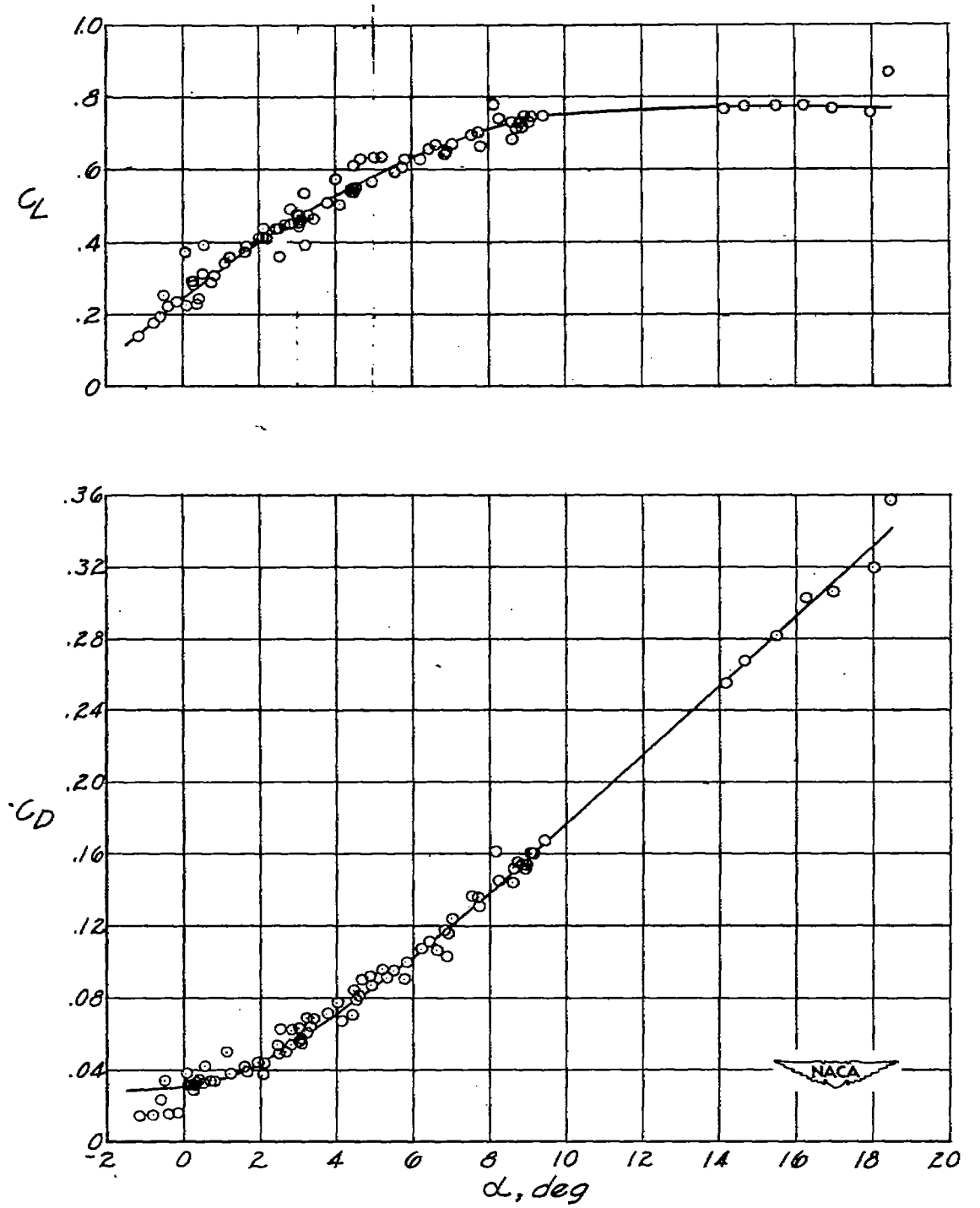

(h) M = 0.83.

Figure 2.- Continued.

[redacted]

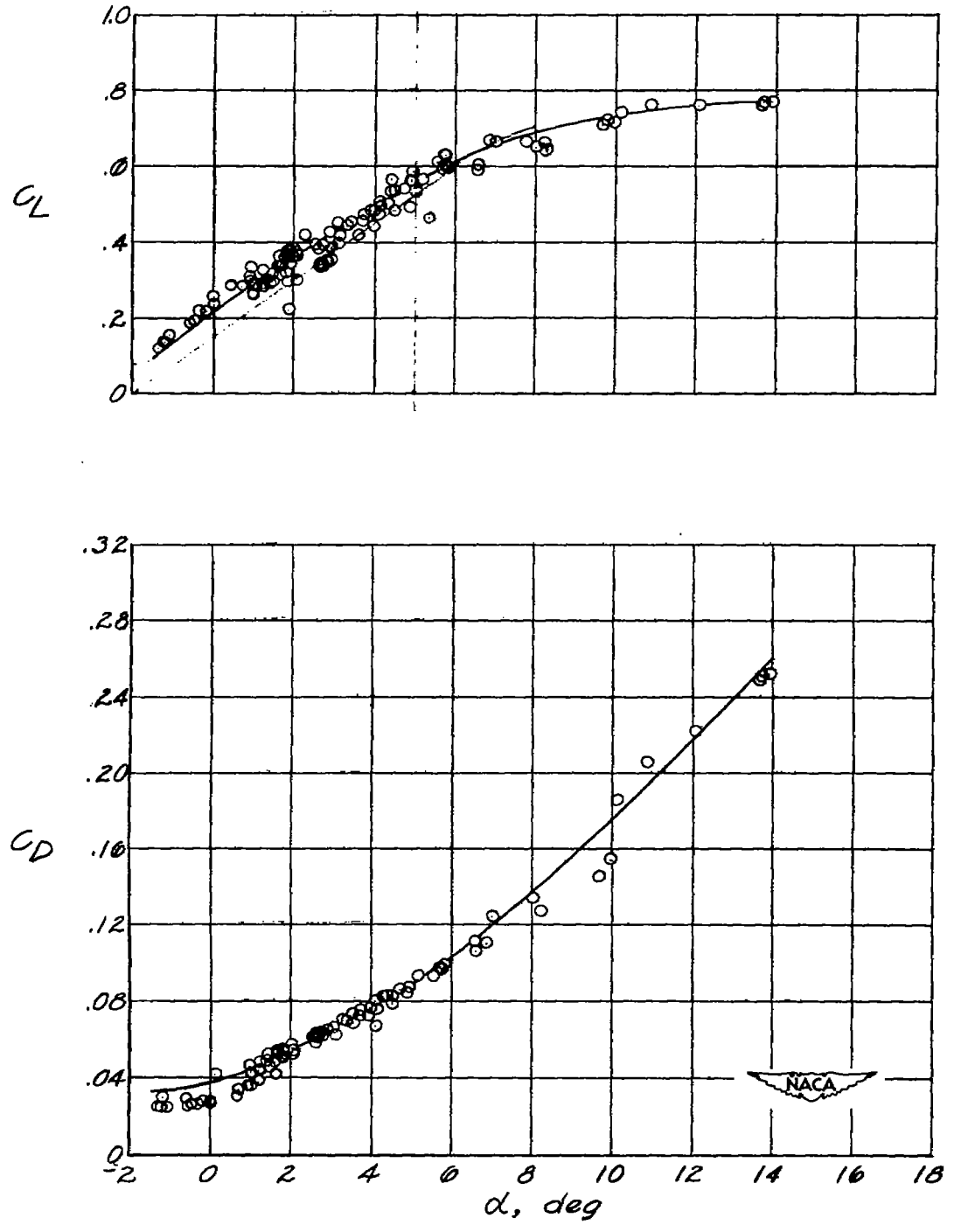

(i) M = 0.85.

Figure 2.- Continued.

[redacted]

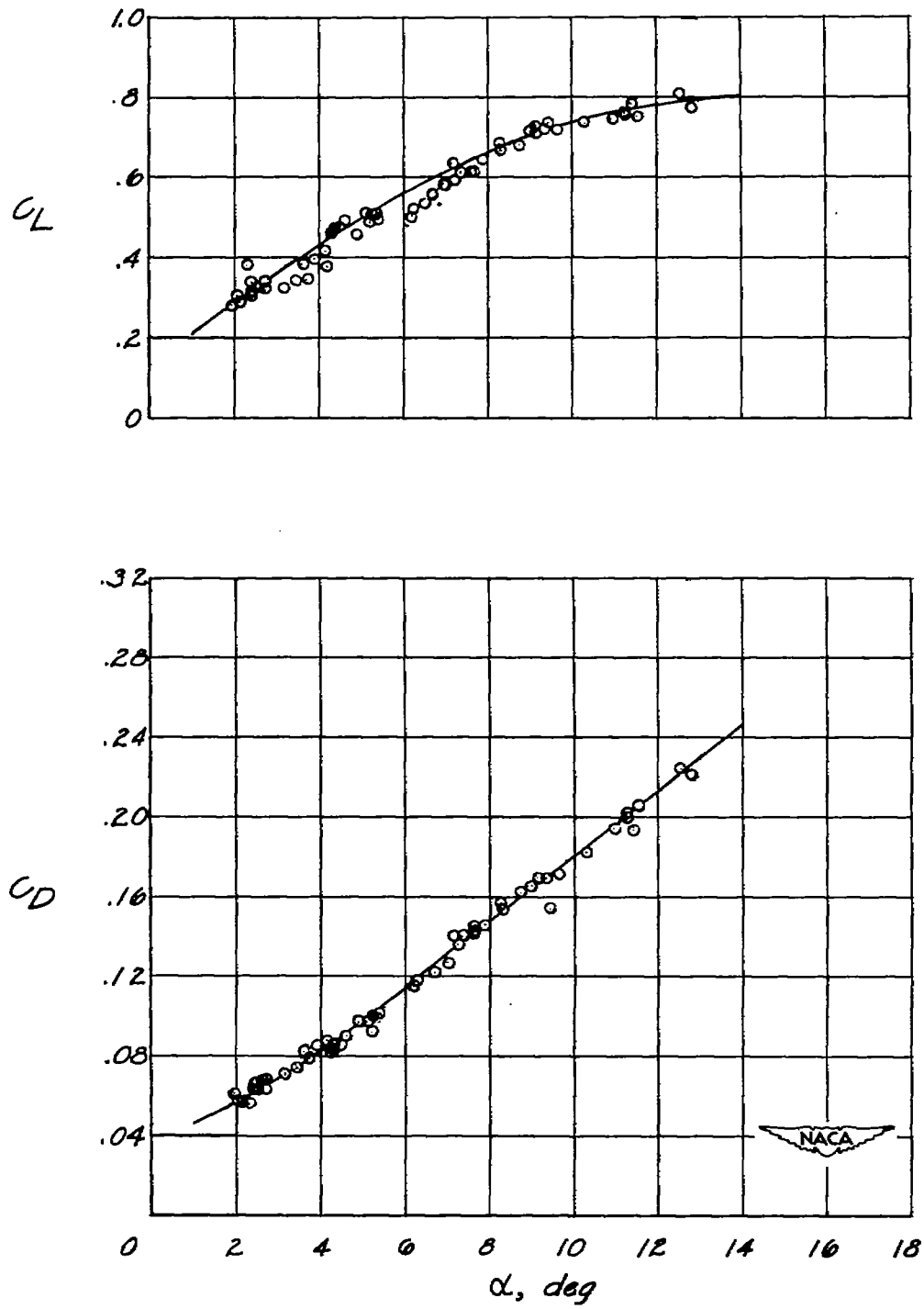

(j) M = 0.87.

Figure 2.- Continued.

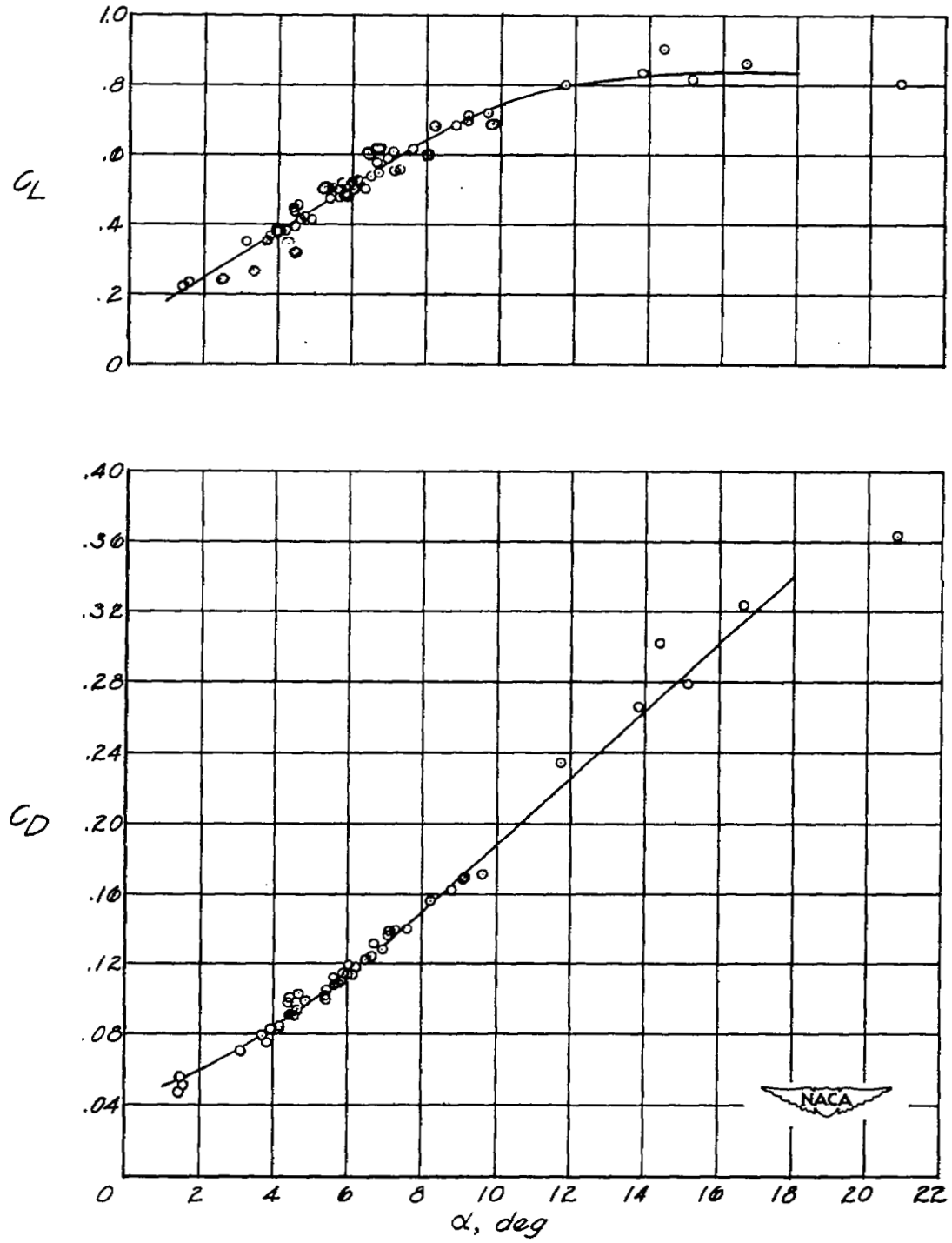

(k) M = 0.89.

Figure 2.- Continued.

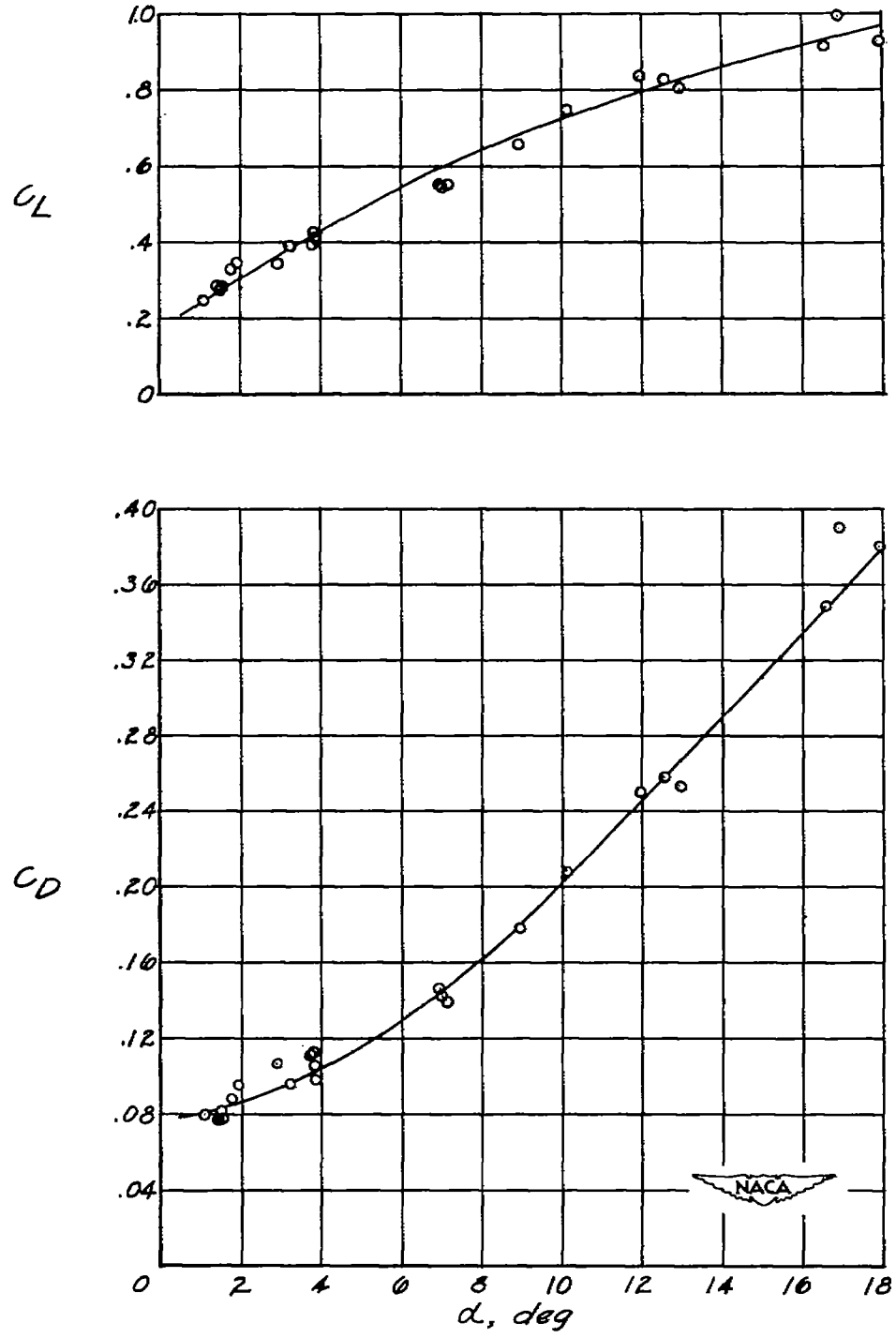

(l) M = 0.91.

Figure 2.- Continued.

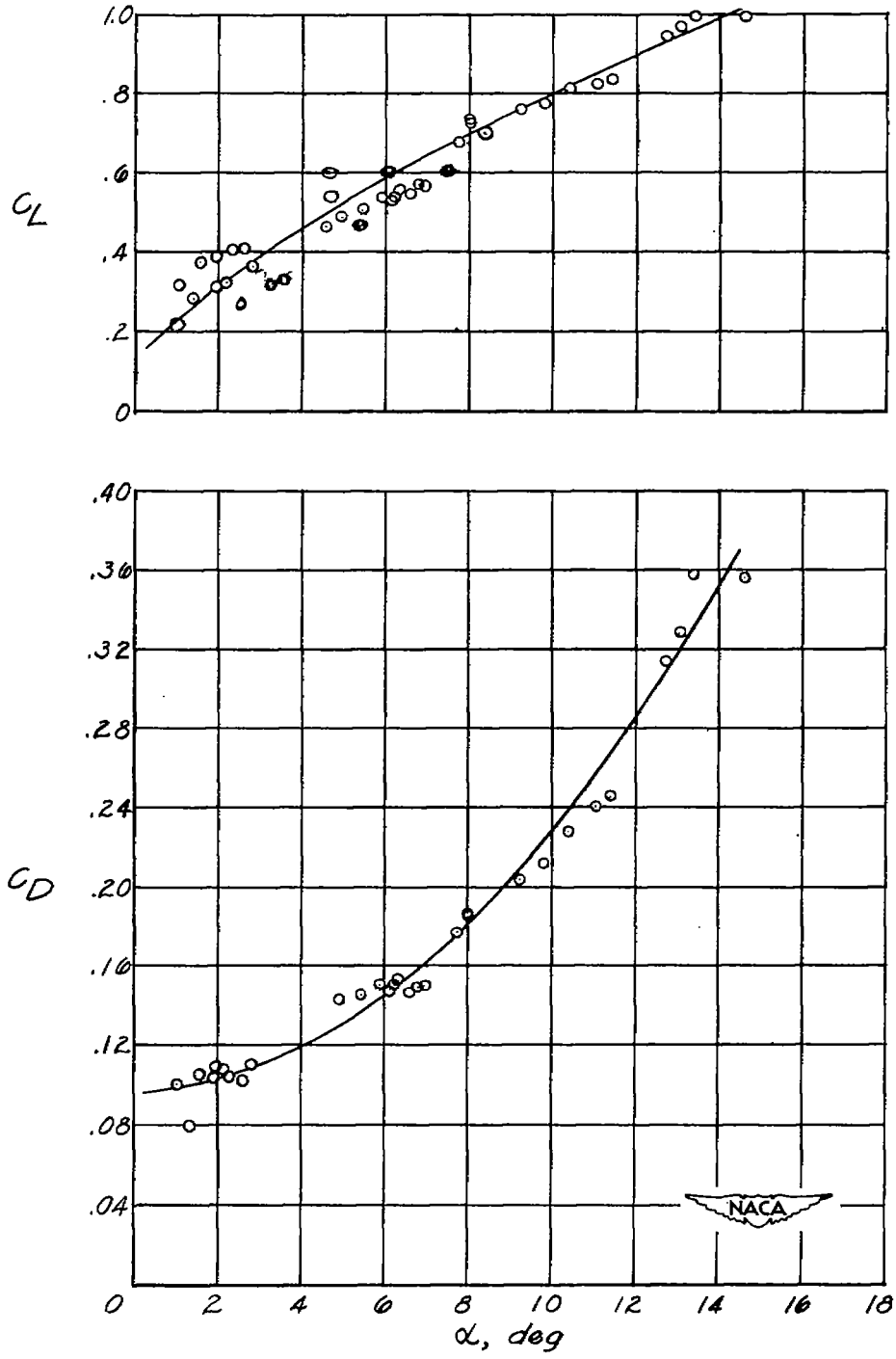

(m) M = 0.93.

Figure 2.- Continued.

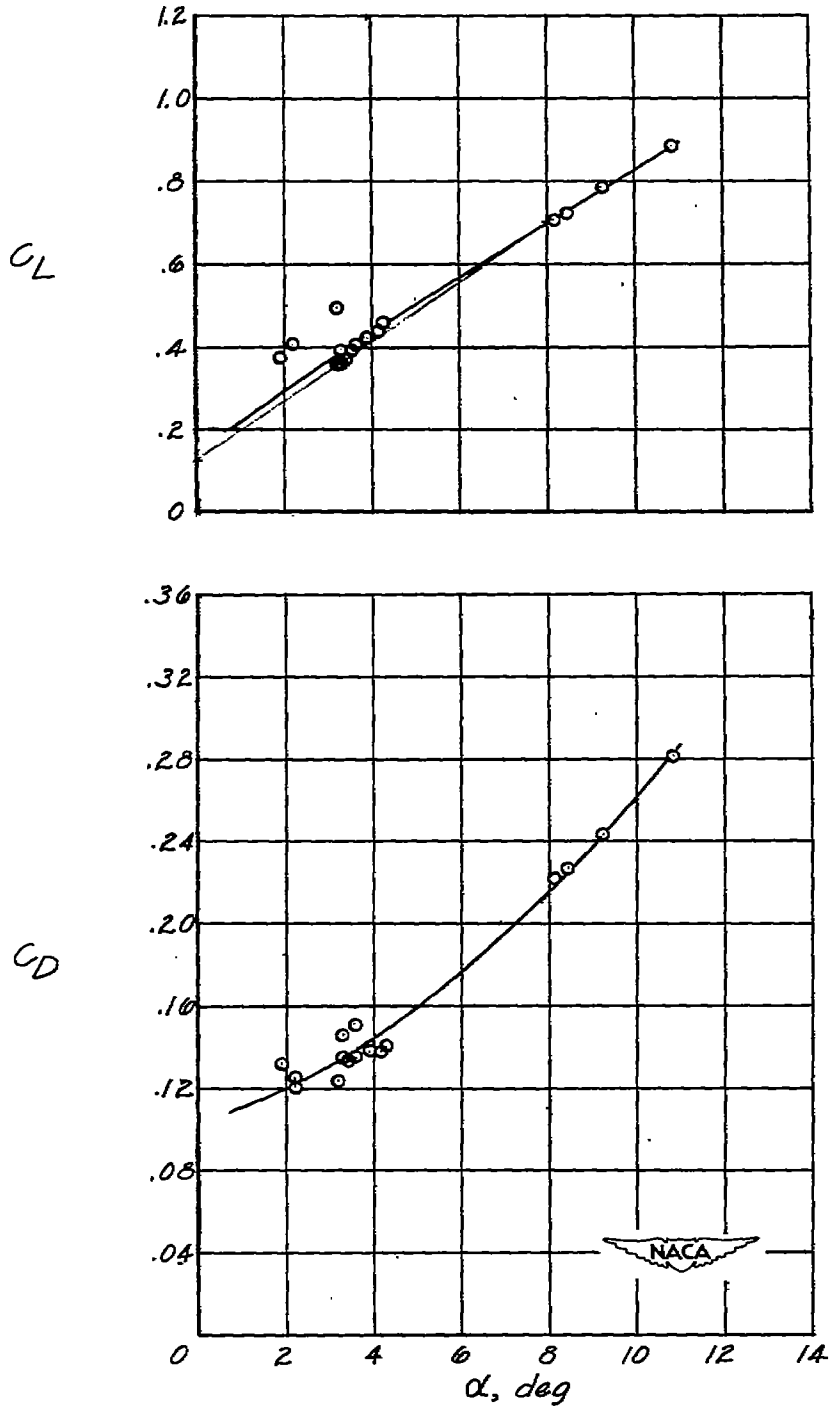

(n) M = 0.97.

Figure 2.- Continued.

[redacted]

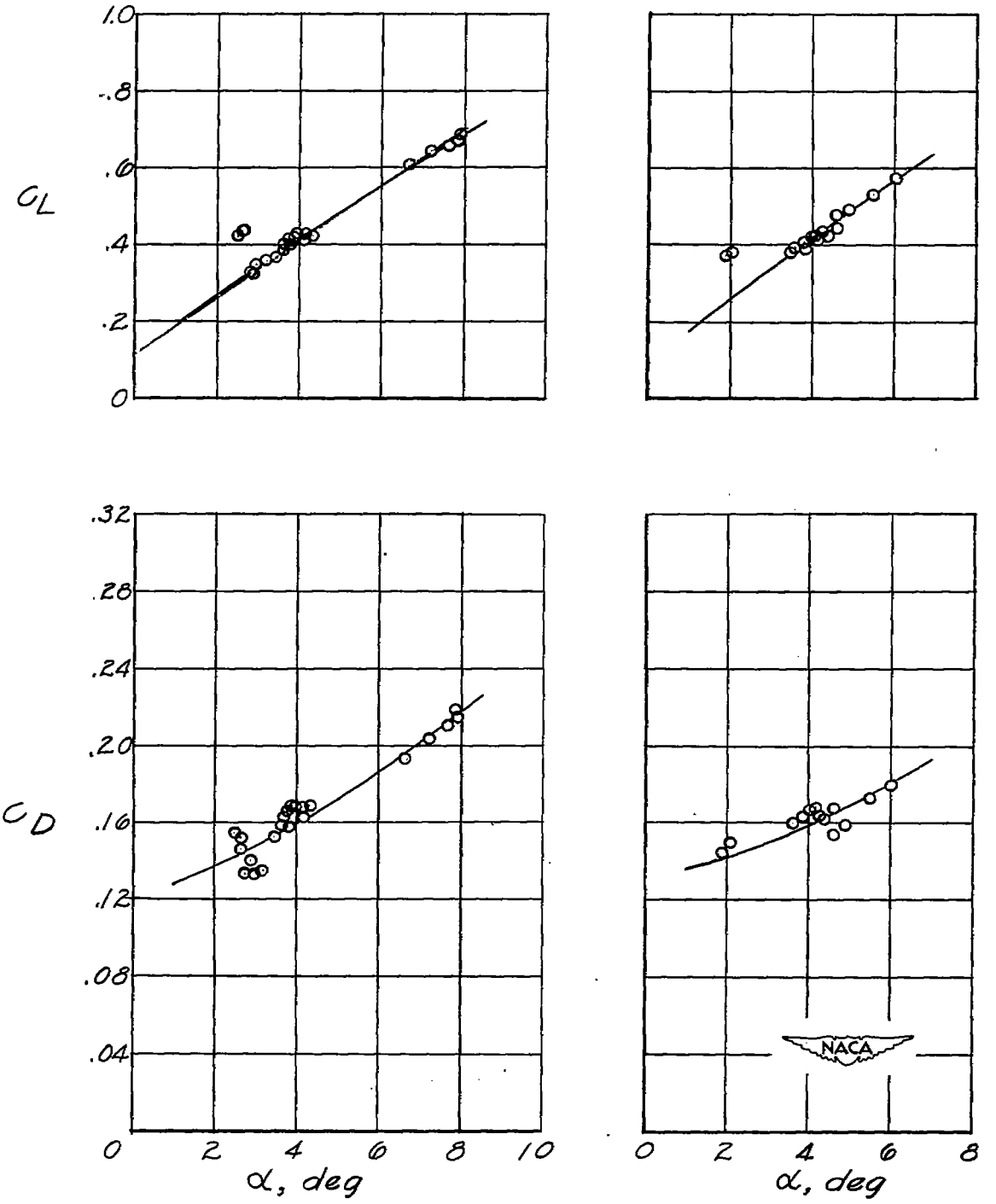

(o) M = 0.99. (p) M = 1.01.

Figure 2.- Concluded.

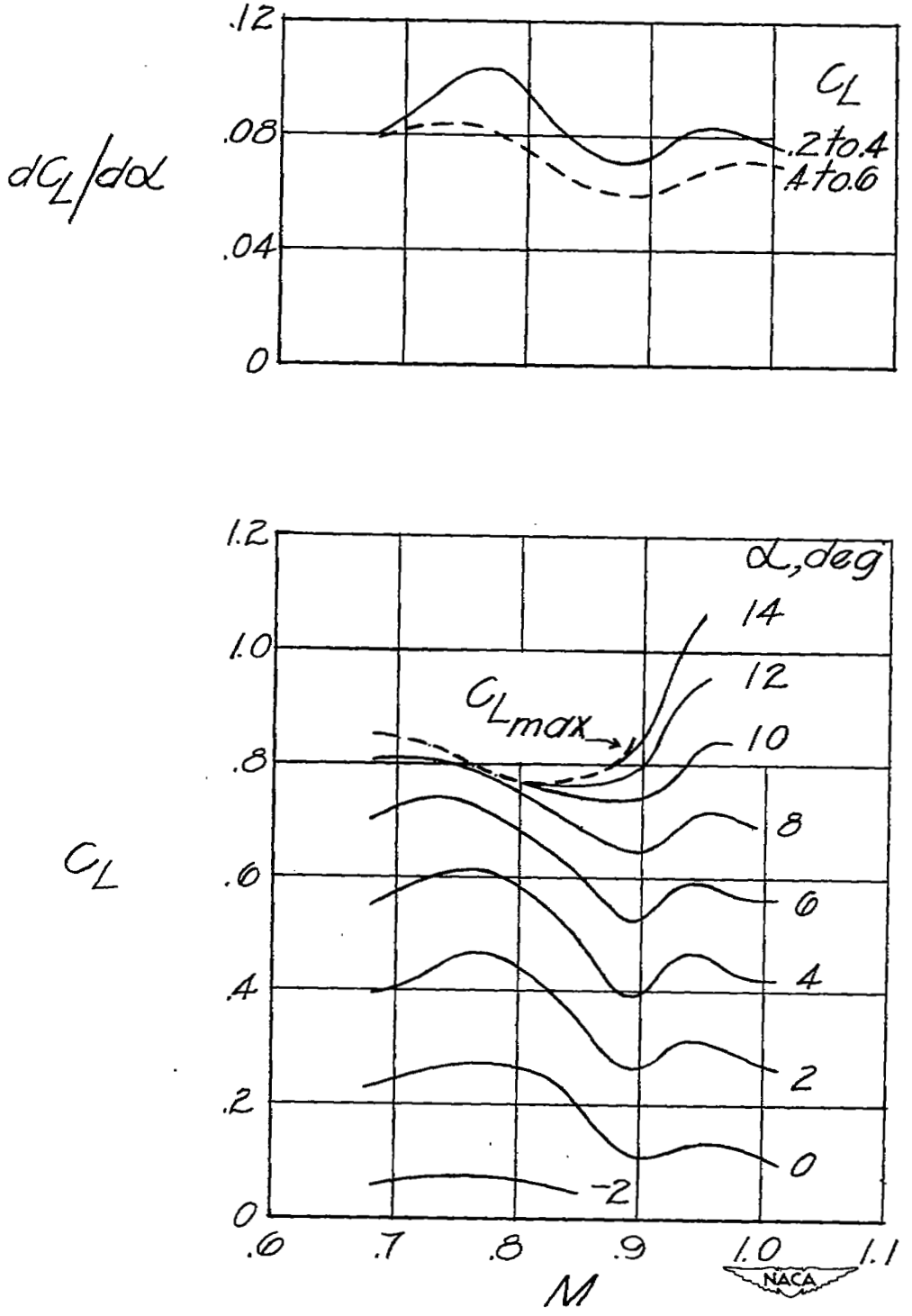

Figure 3.- Variation of lift coefficient and the lift-curve slope with Mach number.

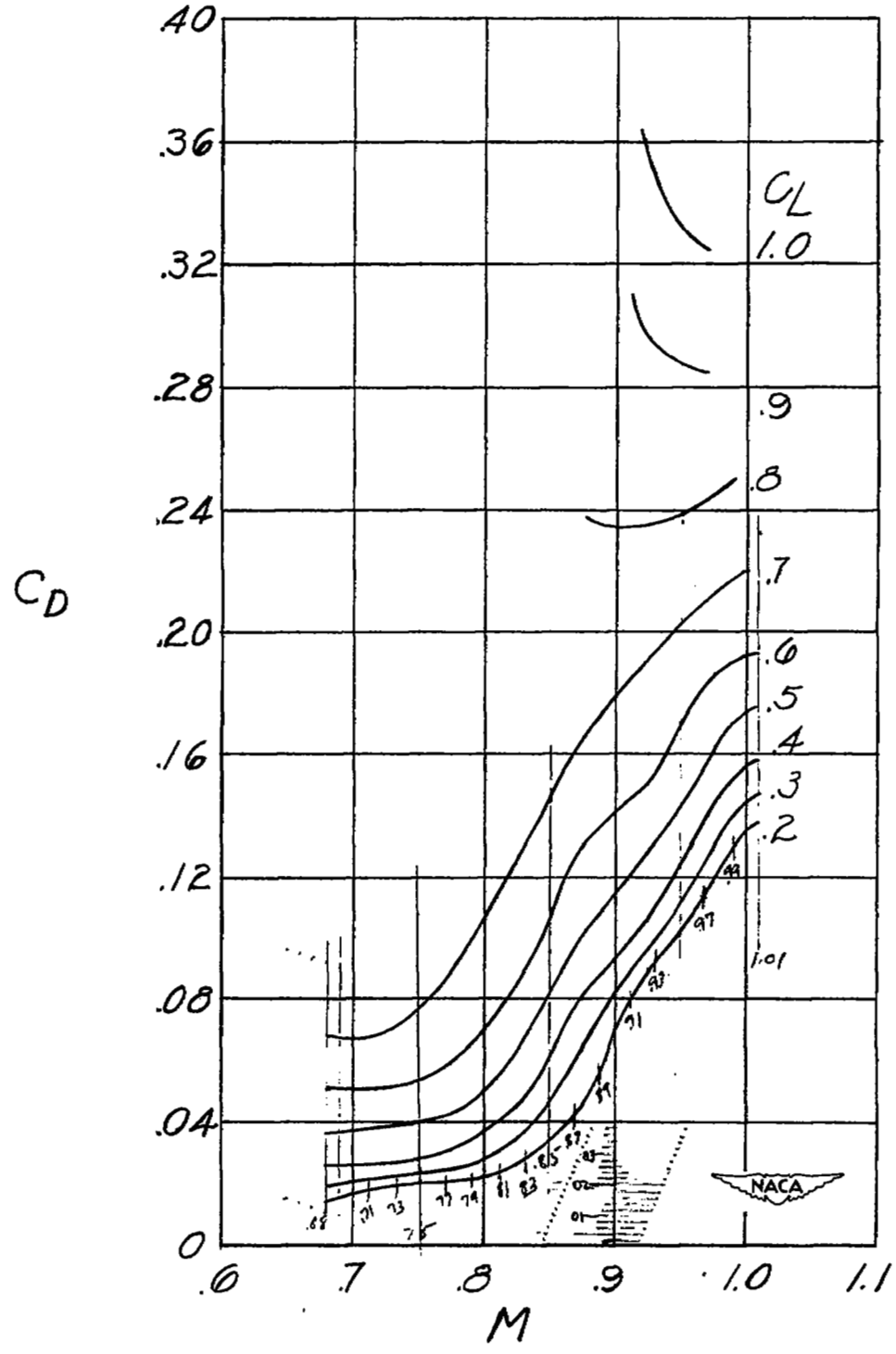

Figure 4.- Variation of drag coefficient with Mach number for constant lift coefficient.

[redacted]

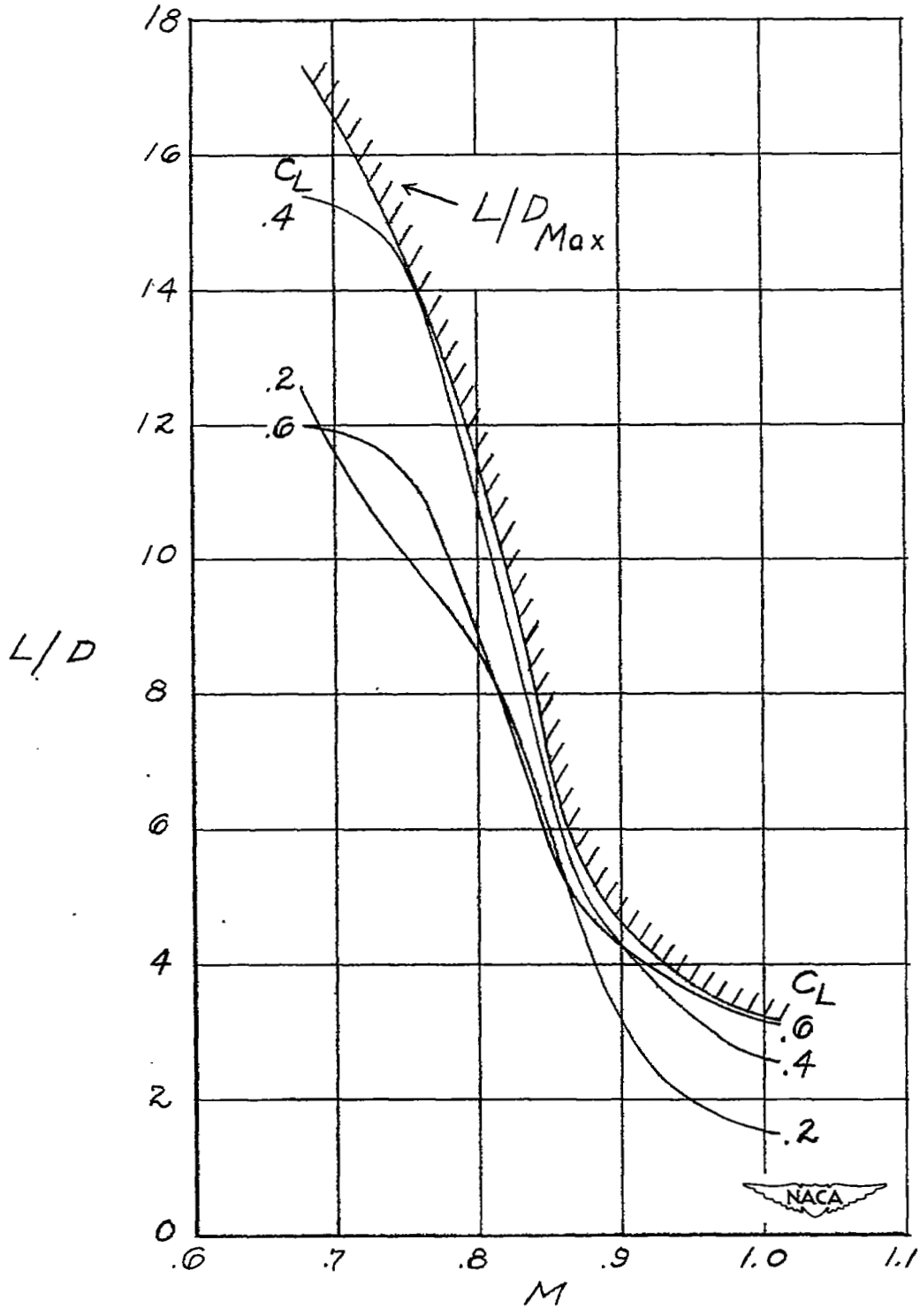

Figure 5.- Variation of lift-drag ratio with Mach number for constant lift coefficient.

[redacted]

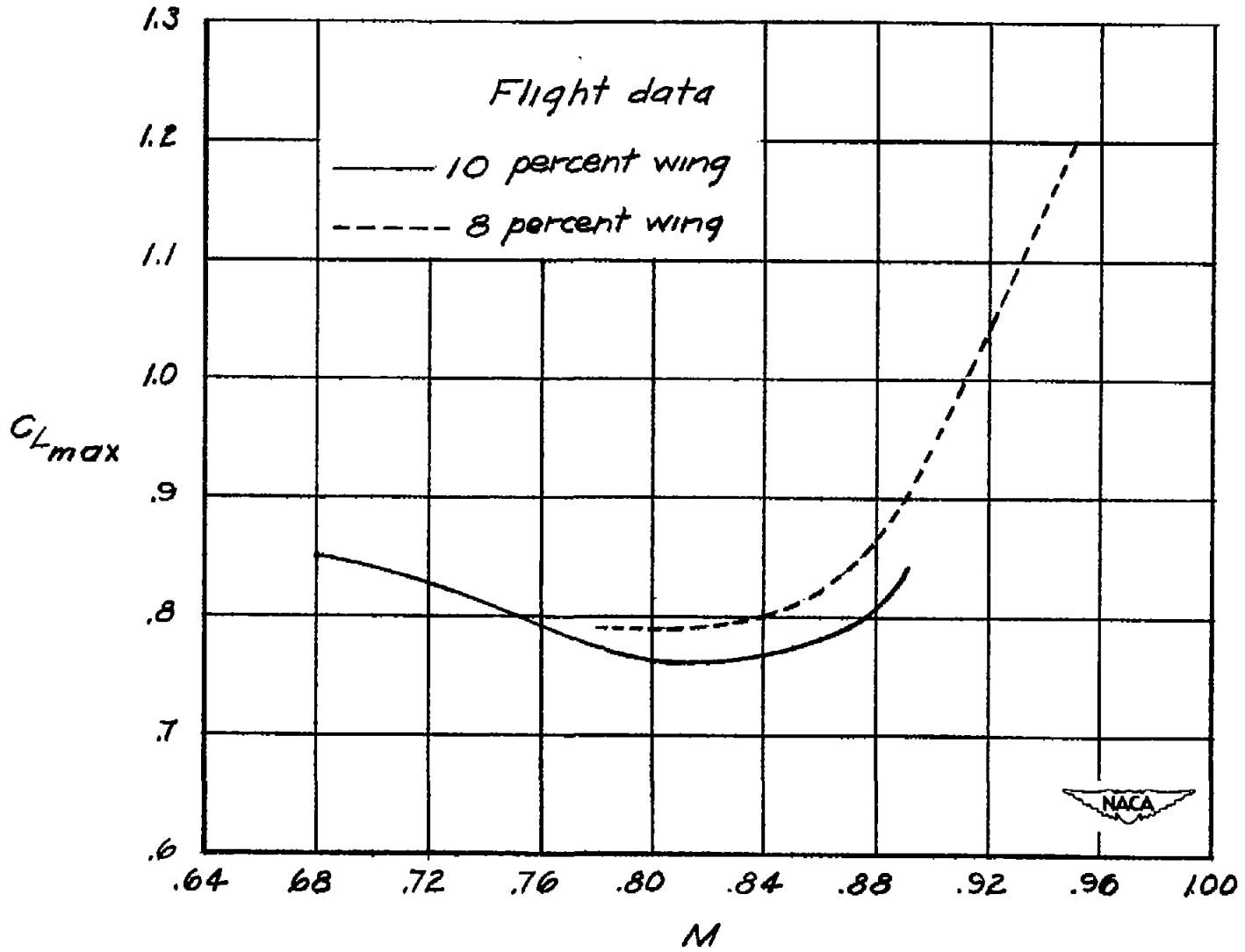

Figure 6.- Variation of maximum lift coefficient with Mach number.

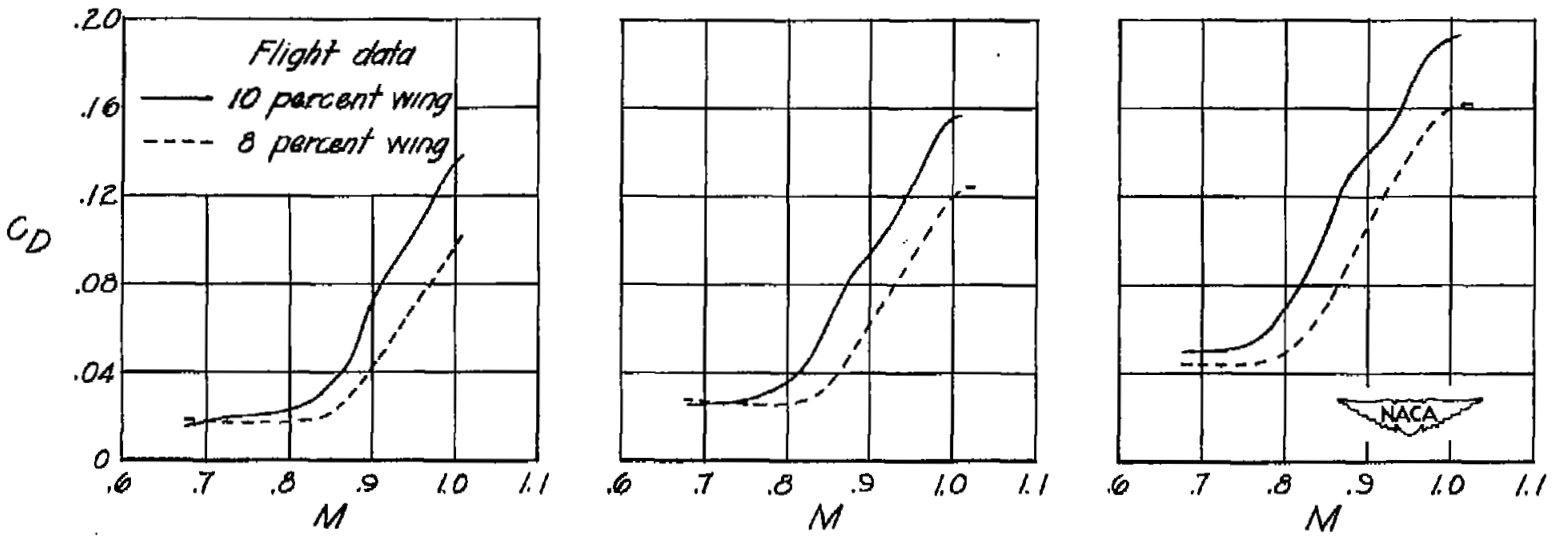

(a) $C_L = 0.2$. (b) $C_L = 0.4$. (c) $C_L = 0.6$.

Figure 7.- Variation of drag coefficient with Mach number for constant lift coefficient.

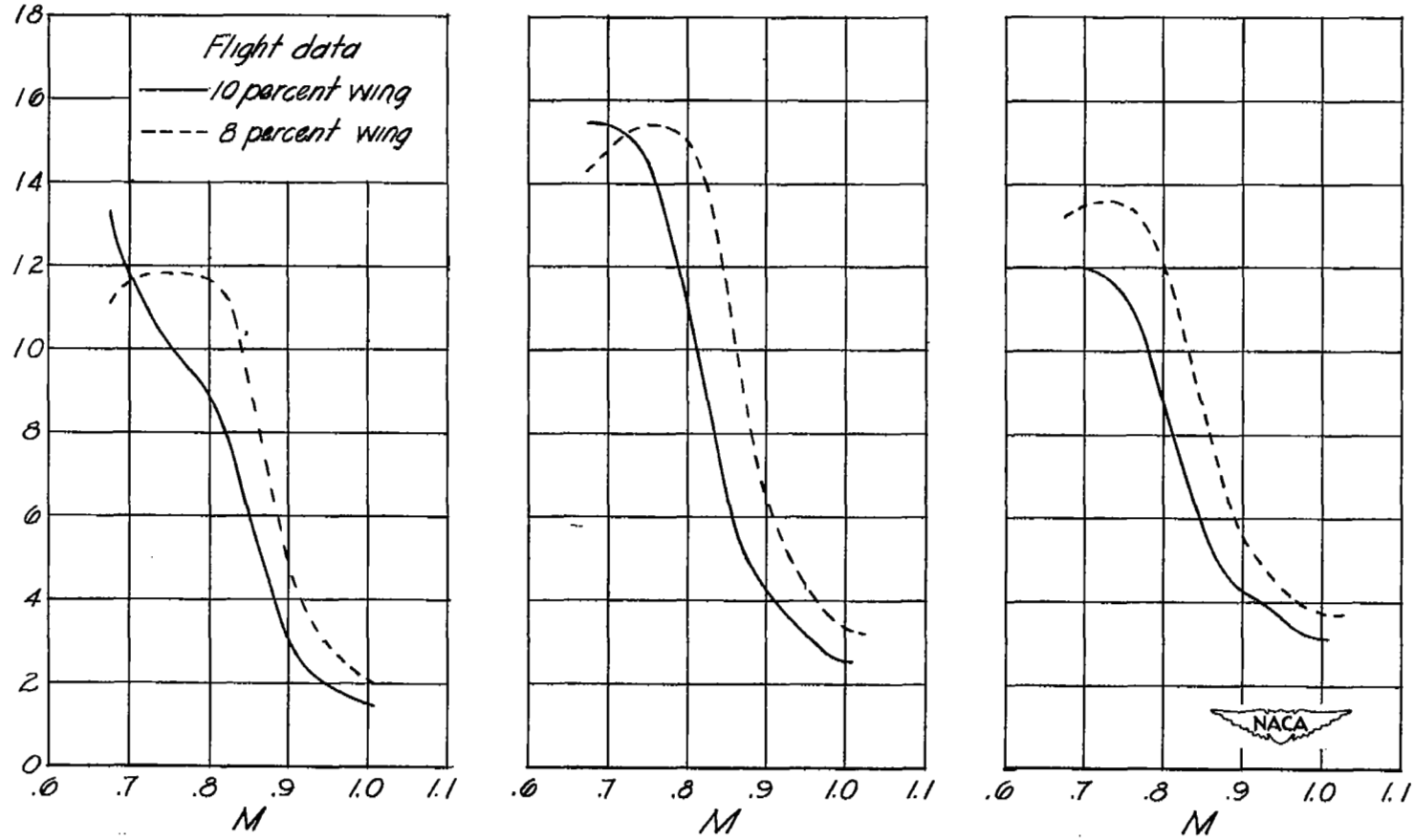

(a) $C_L = 0.2$. (b) $C_L = 0.4$. (c) $C_L = 0.6$.

Figure 8.- Variation of lift-drag ratio with Mach number for constant lift coefficient.

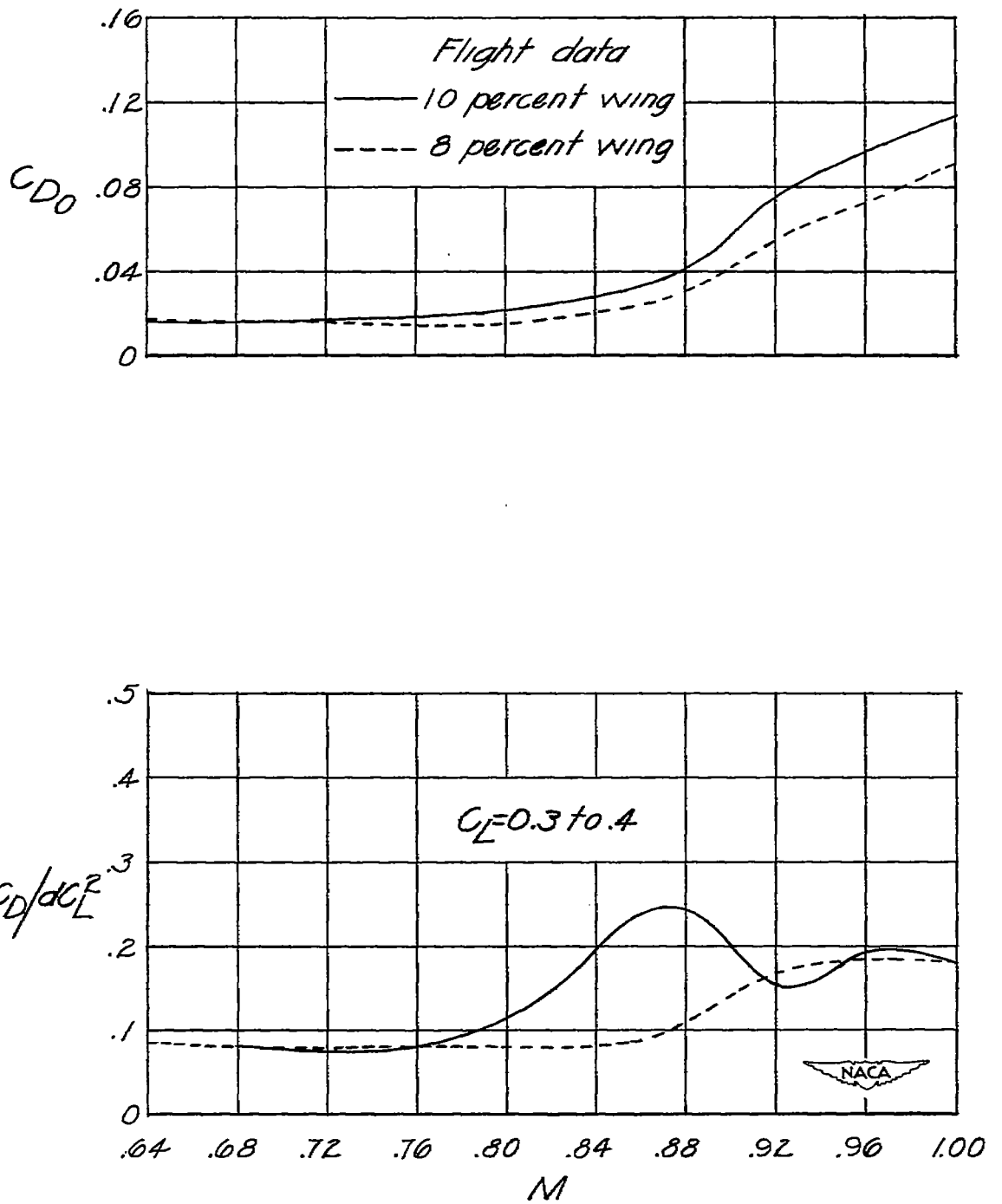

Figure 9.- Variation of drag coefficient at zero lift coefficient and the induced drag factor with Mach number.

[redacted]

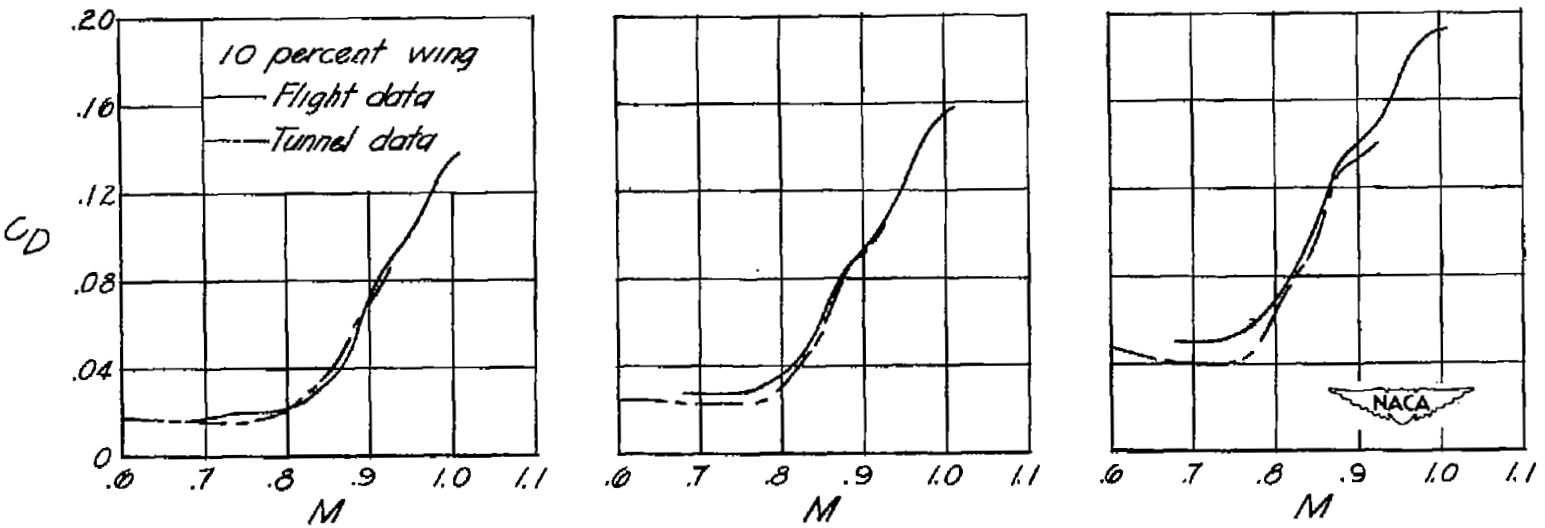

(a) $C_L = 0.2$. (b) $C_L = 0.4$. (c) $C_L = 0.6$.

Figure 10.- Variation of drag coefficient with Mach number for constant lift coefficient.

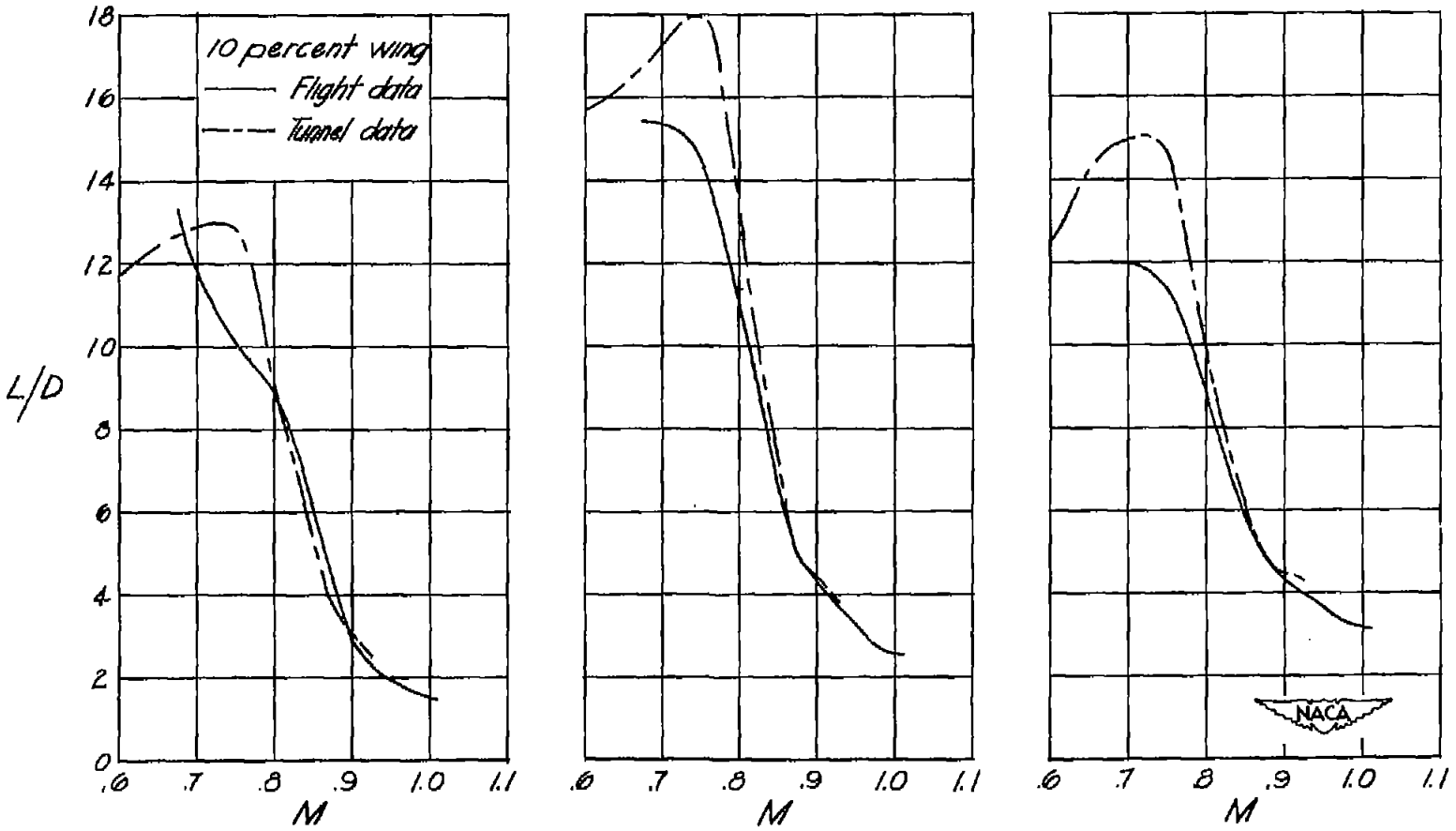

(a) $C_L = 0.2$. (b) $C_L = 0.4$. (c) $C_L = 0.6$.

Figure 11.- Variation of lift-drag ratio with Mach number for constant lift coefficient.

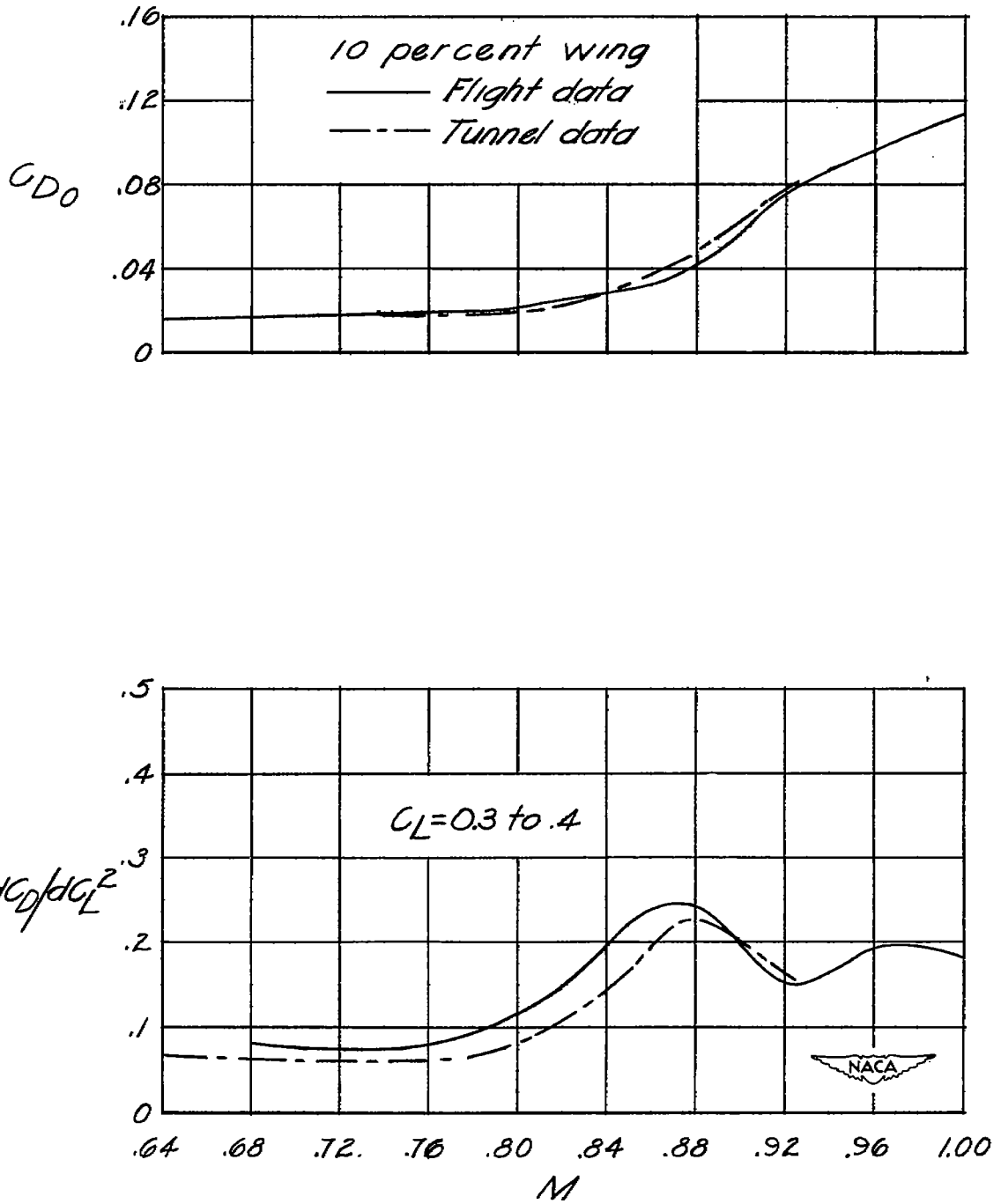

Figure 12.- Variation of drag coefficient at zero lift coefficient and the induced drag factor with Mach number.

[redacted]

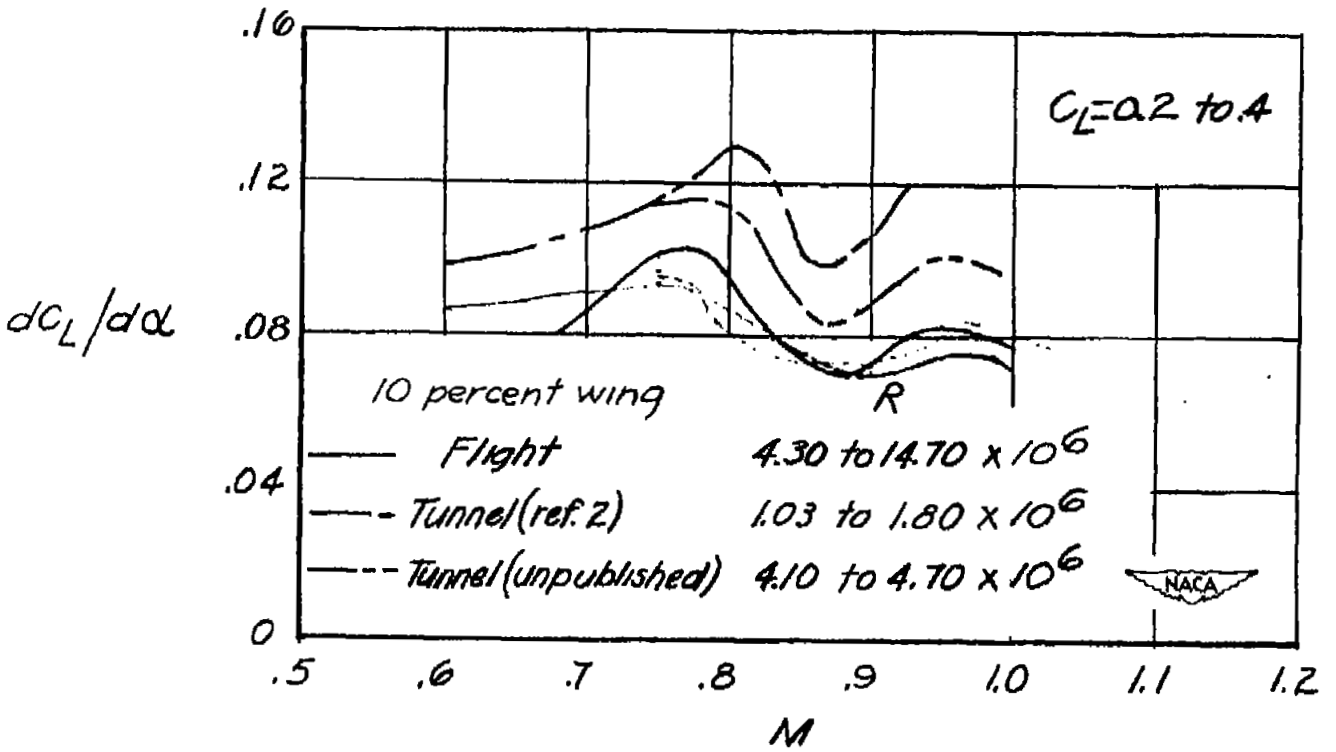

Figure 13.- Variation of lift-curve slope with Mach number.